

(NASA-CR-131845) PLANETARY QUARANTINE.
SPACE RESEARCH AND TECHNOLOGY Semiannual
Review, 1 Jul. - 31 Dec. 1972 (Jet
Propulsion Lab.) 95 p HC \$6.75 CSCL 06M

N73-22039

Unclas

G3/04 69880

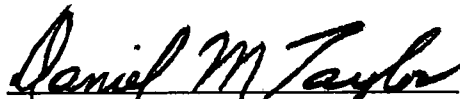
JET PROPULSION LABORATORY
CALIFORNIA INSTITUTE OF TECHNOLOGY
PASADENA, CALIFORNIA

900-608

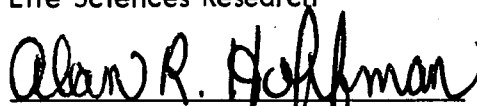
PLANETARY QUARANTINE
Semi-Annual Review
Space Research and Technology

1 July - 31 December 1972

APPROVED BY:



D. M. Taylor, Supervisor
Life Sciences Research



A. R. Hoffman, Supervisor
Planetary Quarantine Analysis



D. S. Hess, Manager
Environmental Requirements Section

JET PROPULSION LABORATORY
CALIFORNIA INSTITUTE OF TECHNOLOGY
PASADENA, CALIFORNIA

ca. May 1973

900-608

CONTENTS

I	PLANETARY QUARANTINE STRATEGIES FOR ADVANCED MISSIONS (NASA No. 193-58-61-01).	1-1
1.1	STRATEGIES FOR SATELLITE ENCOUNTER	1-2
1.1.1	Subtask A Introduction	1-2
1.1.2	Significant Accomplishments	1-2
1.1.3	Conclusions	1-8
1.1.4	Problem Areas	1-8
1.1.5	Future Activities	1-9
1.1.6	Presentations	1-9
1.2	JUPITER ENTRY ANALYSIS	1-9
1.2.1	Subtask B Introduction	1-9
1.2.2	Significant Accomplishments	1-10
1.2.3	Conclusions	1-18
1.2.4	Meaning of Results to Planetary Quarantine	1-19
1.2.5	Future Activities	1-20
1.2.6	Presentations	1-20
II	NATURAL SPACE ENVIRONMENT STUDIES (NASA No. 193-58-61-02)	2-1
2.1	EFFECT OF PLANETARY TRAPPED RADIATION BELT ON MICROORGANISMS	2-2
2.1.1	Subtask A Introduction	2-2
2.1.2	Significant Accomplishments.	2-2
2.1.3	Future Activities	2-2
2.2	EFFECT OF SOLAR WIND RADIATION ON MICROORGANISMS	2-3
2.2.1	Subtask B Introduction	2-3
2.2.2	Significant Accomplishments.	2-3
2.2.3	Future Activities	2-3
2.3	EFFECT OF SPACE VACUUM ON MICROORGANISMS	2-3
2.3.1	Subtask C Introduction	2-3

CONTENTS (contd)

2.3.2	Significant Accomplishments	2-4
2.3.3	Problem Areas	2-11
2.3.4	Future Activities	2-11
2.3.5	Presentations	2-11
2.4	PROBABILITY OF GROWTH IN PLANETARY ATMOSPHERES AND SATELLITES	2-12
2.4.1	Subtask D Introduction.	2-12
2.4.2	Significant Accomplishments	2-12
2.4.3	Relevance to Planetary Quarantine	2-19
2.4.4	Future Activities	2-20
2.4.5	Presentation.	2-20
2.4.6	References.	2-20
III	POST LAUNCH RECONTAMINATION STUDIES (NASA No. 193-58-62-03)	3-1
3.1	POST LAUNCH RECONTAMINATION STUDIES	3-2
3.1.1	Subtask A Introduction.	3-2
3.1.2	Significant Accomplishments	3-2
3.1.3	Future Activities	3-2
IV	SPACECRAFT CLEANING AND DECONTAMINATION TECHNIQUES (NASA No. 193-58-67-02).	4-1
4.1	PHYSICAL REMOVAL OF SPACECRAFT MICROBIAL BURDEN.	4-2
4.1.1	Subtask A Introduction.	4-2
4.1.2	Significant Accomplishments	4-2
4.1.3	Future Activities	4-2
4.2	VERIFICATION OF USSR HYDROGEN PEROXIDE DECONTAMINATION DATA	4-2
4.2.1	Subtask B Introduction.	4-2
4.2.2	Approach	4-3
4.2.3	Significant Accomplishments	4-3
4.2.4	Future Activities	4-4
4.2.5	Presentation.	4-4

CONTENTS (contd)

4.3	EVALUATION OF PLASMA CLEANING AND DECONTAMINATION TECHNIQUES	4-6
4.3.1	Subtask C Introduction.	4-6
4.3.2	Significant Accomplishments	4-6
4.3.3	Future Activities	4-6
4.3.4	Presentation.	4-7
V	PROBABILITY ESTIMATION METHODS AND ANALYSIS (NASA No. 193-58-63-04)	5-1
5.1	SUBTASK A INTRODUCTION.	5-2
5.2	SIGNIFICANT ACCOMPLISHMENTS	5-2
5.2.1	Critique of Analytical Approaches Used for Determination of Planetary Quarantine Parameters and Probabilities.	5-2
5.2.2	Approach for Microbial Burden Prediction.	5-13
5.2.3	Approach for Analyzing the Vacuum Temperature Data.	5-18
5.2.4	Theoretical Formulation for Planetary Quarantine Standards	5-19
5.3	CONCLUSIONS	5-19
5.4	PROBLEM AREAS	5-20
5.5	FUTURE ACTIVITIES.	5-20
5.6	PRESENTATIONS.	5-20
5.7	PUBLICATIONS.	5-20
5.8	REFERENCES	5-21
	APPENDIX A - ANALYTICAL APPROACH FOR ANALYZING OF THE VACUUM TEMPERATURE DATA	A-1

TABLES

1-A.1	Maximum Titan impact probabilities for a closest approach distance of 10,000 km.	1-4
1-A.2	1 σ Total delivery errors in Saturn aim plane for post-Jupiter midcourse correction maneuvers.	1-5
2-C.1	Effect of vacuum at 25°C on spore activation.	2-5
2-C.2	Log reduction of spacecraft isolates	2-10
2-D.1	Chemical components of icy satellites	2-16
2-D.2	Significant properties of satellites considered in the P _g analysis	2-18
4-B.1	Percent survival of spores exposed to hydrogen peroxide	4-5
4-B.2	Percent survival of vegetative cells exposed to hydrogen peroxide.	4-5

FIGURES

1-A.1	Satellite encounter geometry	1-3
1-A.2	Satellite encounter flyby geometry	1-4
1-A.3	Satellite impact probability strongly a function of satellite closest approach and flyby geometry	1-6
1-A.4	Titan impact probabilities for various flyby designs, Maneuver 4	1-7
1-A.5	Titan impact probabilities for various flyby designs, Maneuver 6	1-7
1-B.1	Thermal corridors for plastic particles	1-11
1-B.2	Typical thermal response of blankets, outer planets spacecraft -- nominal atmosphere	1-12
1-B.3	Antenna geometry	1-14
1-B.4	Antenna temperatures at continuum flow, boundary face orientation - non ablating structure	1-14
1-B.5	Antenna temperatures at entry into continuum, edge orientation -- non ablating structure	1-15
1-B.6	Disintegration stages of outer planets spacecraft	1-19
2-C.1	Vacuum temperature resistance of spores of spacecraft isolates	2-8
2-C.2	Vacuum temperature resistance of nonsporeforming spacecraft isolates	2-8
2-D.1	pH values vs temperature in highest P_g regions of Jupiter model atmospheres	2-14
2-D.2	Pressure vs temperature for the Saturn model atmospheres	2-15
2-D.3	Temperature profiles of icy satellites (No atmosphere)	2-16
2-D.4	Relative probabilities of growth for Jupiter, Saturn and their satellites	2-19
4-B.1	Hydrogen peroxide test procedure	4-4
5-A.1	Schematic representation of contamination probability equation	5-2

SECTION I

PLANETARY QUARANTINE STRATEGIES
FOR
ADVANCED MISSIONS
(NASA No. 193-58-61-01)

Contents

Subtask A
para. 1.1

Title and Related Personnel

STRATEGIES FOR SATELLITE ENCOUNTER

Cognizance: C. Gonzalez

Associate

Personnel: W. Stavro, C. Lefkowitz

Subtask B
para. 1.2

JUPITER ENTRY ANALYSIS

Cognizance: C. Gonzalez,

Associate

Personnel: W. Jaworski, A. McDonald,
W. Stavro

1.1 STRATEGIES FOR SATELLITE ENCOUNTER

1.1.1 Subtask A Introduction

The objectives of this task are:

- 1) Determine the implication of satisfying quarantine constraints on current outer planet mission and spacecraft designs and;
- 2) Develop tools required to perform trajectory and navigation analysis for determining satellite impact probabilities.

To date the required software for determining satellite impact probabilities has been completed. An application of this software to a mission with a Titan (satellite of Saturn) encounter has also been completed.

The work described here is considered especially timely in that both the Mariner Jupiter/Saturn and the Pioneer Jupiter missions are planning satellite encounters. In addition, recent data has been released which predicts a green house effect on Titan*.

1.1.2 Significant Accomplishments

Two typical outer planet trajectories were considered as involving satellite encounters. The satellite encounter geometry for these trajectories is shown in Fig. 1-A.1. Two spacecraft will be launched. The first one encountering the satellites, Io (Jupiter) and Titan. The second one will be launched with an optional satellite encounter at Saturn. The options include encountering Tethys or Titan. The choice depends on the success of the first encounter with Titan. The decision is made any time during the Jupiter-Saturn leg, but prior to 60 days before Saturn encounter. A mission with an optional trajectory, to be selected after launch, has not been previously investigated from the viewpoint of satisfying quarantine requirements.

Two factors must be considered in order to determine the probability of impacting a given satellite. One of these is the area in the aim plane of the

*Berkman, R., "Probability of Growth in Planetary Atmospheres and Satellites," presented at the Semi Annual NASA Sterilization Technology Seminar, New Orleans, Louisiana, January 30-31, 1973.

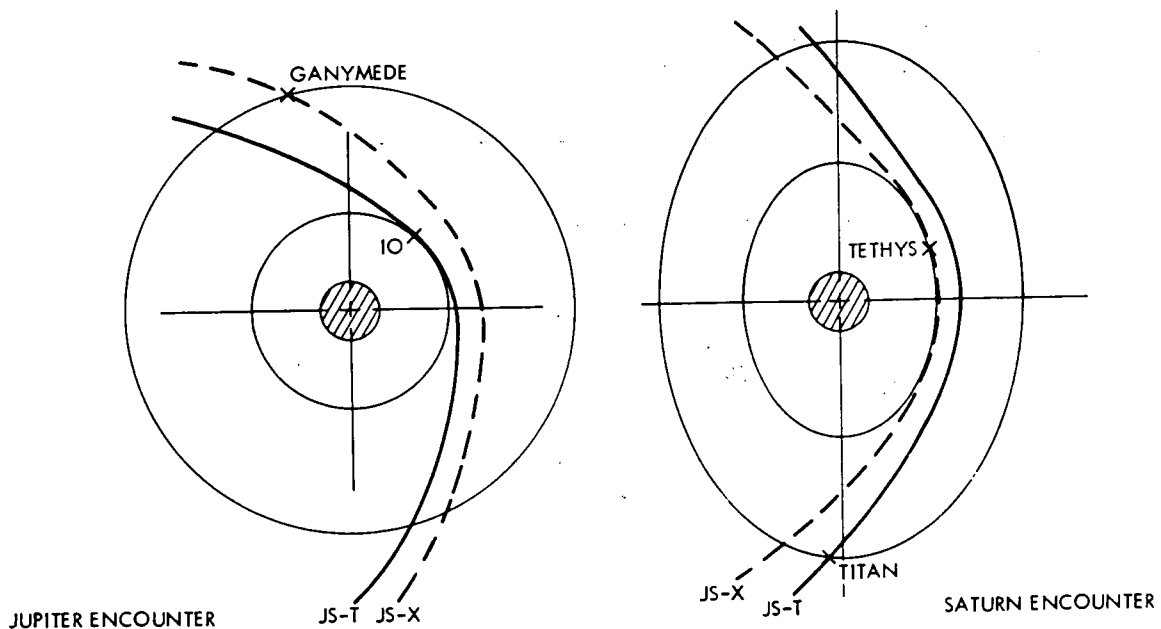


Fig. 1-A.1 Satellite encounter geometry

encounter planet that would result in impact by a spacecraft passing through this area. The satellite, itself, may be located anywhere in three dimensional space around the planet. The second factor is the dispersion of errors of the correction maneuver in question. This dispersion is represented by an ellipse in the aim plane, such that there is a given probability of finding the spacecraft anywhere in that ellipse, when it crosses the aim plane. The situation is shown in Fig. 1-A.2.

In order to determine the probability of impact, a numerical integration of a bivariate Gaussian distribution (representing the dispersion errors) is performed over the impact area, using a computer routine. Since a quarantine analysis had not been performed previously for a satellite encounter case, tools were developed to determine the impact area and to perform the numerical integration. This tool development was the major part of the first six month's effort.

The tools developed were used to determine the probability of impacting Titan using typical outer planet trajectories selected from proposed Mariner Jupiter/Saturn missions. The probabilities were determined for various distances of closest approach (DCA). Table 1-A.1 gives the maximum impact

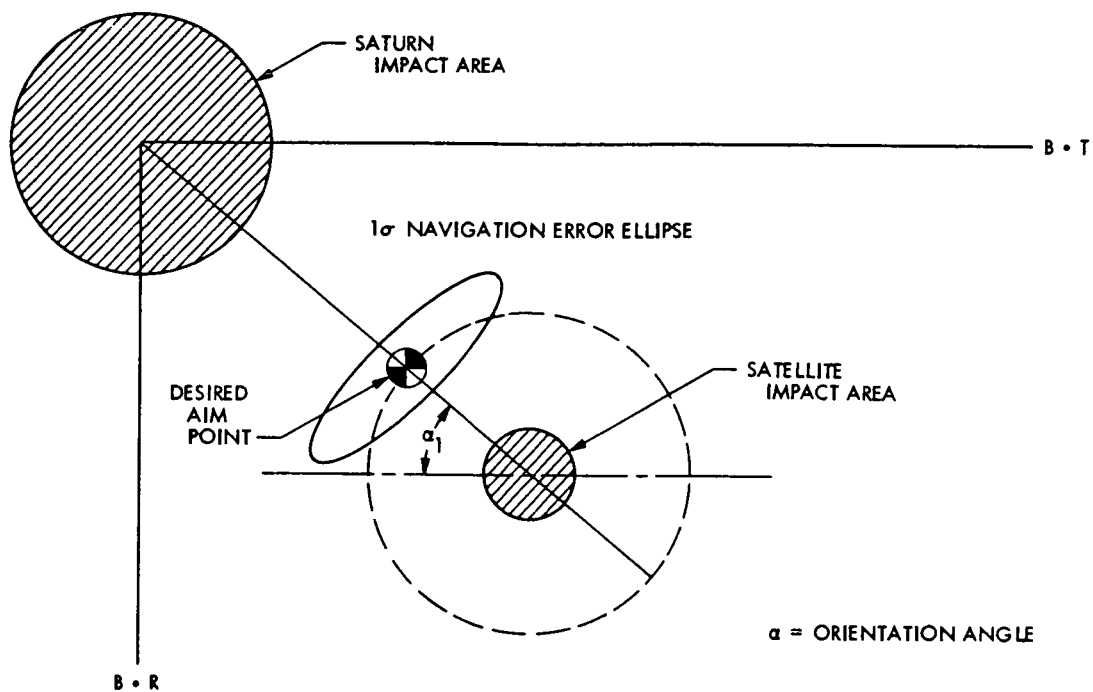


Fig. 1-A.2 Satellite encounter flyby geometry

Table 1-A.1 Maximum Titan impact probabilities for a closest approach distance of 10,000 km

Maneuver	P_{Imp}	P_I^*
Maneuver 3 (Pre-Jupiter)	10^{-6}	10^{-8}
Maneuver 4 (Post-Jupiter)	1.8×10^{-2}	$\approx 1.0 \times 10^{-4}$
Maneuver 5 (1st Pre-Saturn)	2.2×10^{-4}	$\approx 1.0 \times 10^{-6}$
Maneuver 6 (2nd Pre-Saturn)	1.1×10^{-4}	1.1×10^{-4}
* Assuming $P_{\text{mm}} \approx 1 \times 10^{-2}$ $P_I = P_{\text{Imp}} P_{\text{mm}}$		

probabilities for maneuvers 3 - 6 for a DCA of 10,000 km. The first column gives the probability, P_{Imp} , of the spacecraft impacting the satellite due to the dispersion errors of the maneuver. However, if a subsequent correction maneuver is planned, one minus the probability of being able to perform this maneuver in order to change the impact trajectory, must be factored in. Let this probability be P_{mm} . This number is of the order of magnitude of 10^{-2} . Therefore:

$$P_I = P_{\text{Imp}} P_{\text{mm}}$$

where P_I is the probability of impacting the satellite, taking into account the probability of being able to perform a subsequent convection maneuver. Column two gives the values of P_I (using $P_{\text{mm}} = 10^{-2}$). If a quarantine constraint of 6.4×10^{-5} is assumed*, it is seen that maneuvers 4 and 6 could result in a quarantine violation. $P_{\text{mm}} = 1$ for maneuver 6, since no subsequent maneuver is planned.

An interesting fact is noted when considering the geometry of the dispersion ellipses for maneuvers 4 and 6. Table 1-A.2 gives the geometric parameters for these figures. When the numbers in the two columns differ considerably the ellipses are eccentric. Considering the critical maneuvers, 4 and 6, maneuver 4 has essentially a circular dispersion figure; while maneuver 6 has one which is eccentric.

Table 1-A.2 1σ Total delivery errors in Saturn aim plane for post-Jupiter midcourse correction maneuvers

Maneuver	$\sigma B \cdot R$	$\sigma B \cdot T$
4	4,037 km	4,233 km
5	651 km	2,123 km
6	414 km	2,000 km

*The quarantine allocation given to Pioneer F&G.

Figure 1-A.3 illustrates why this is important. The dispersion ellipse is shown in two positions. The positions are distinguished by using an arbitrary reference line passing through the center of the impact circle. An angle, the orientation angle, between this line and a line connecting the aim point and the center of the impact circle gives the position of the aim point (and consequently the dispersion ellipse) relative to the arbitrary reference. In Figure 1-A.3, when the dispersion ellipse is positioned as given by α_1 , there is no overlap with the impact circle; in the position given by α_2 there is overlap. In both cases the distance from the aim point to the center of the impact circle is the same. However, in the first case, the probability of impact is nil, while in the second case it would be a finite value which could lead to a quarantine violation. Note, that if the 1σ navigation error were circular instead of elliptical a difference in orientation would make no difference in the probability of impact.

The variation of the probability of impact with orientation of the aim point for maneuvers 4 and 6 is illustrated in Fig. 1-A.4 and 1-A.5. In Fig. 1-A.4, the probability of impact (due to maneuver 4) is plotted vs orientation angle for various encounter distances. It is seen that there is little variability,

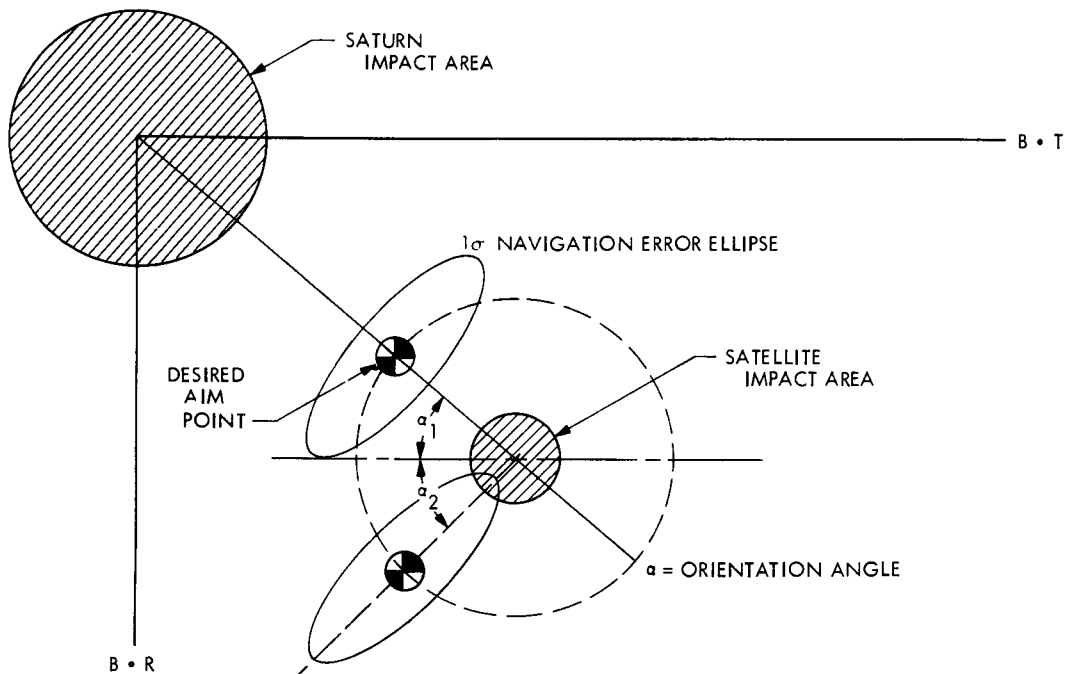


Fig. 1-A.3 Satellite impact probability strongly a function of satellite closest approach and flyby geometry

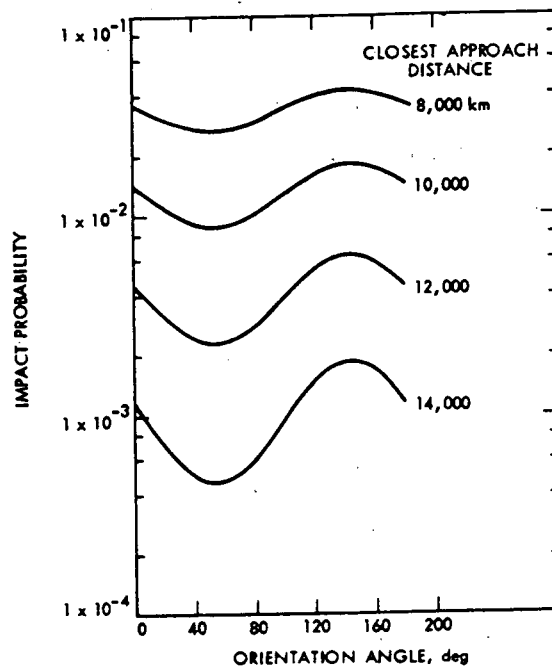


Fig. 1-A.4 Titan impact probabilities for various flyby designs, Maneuver 4

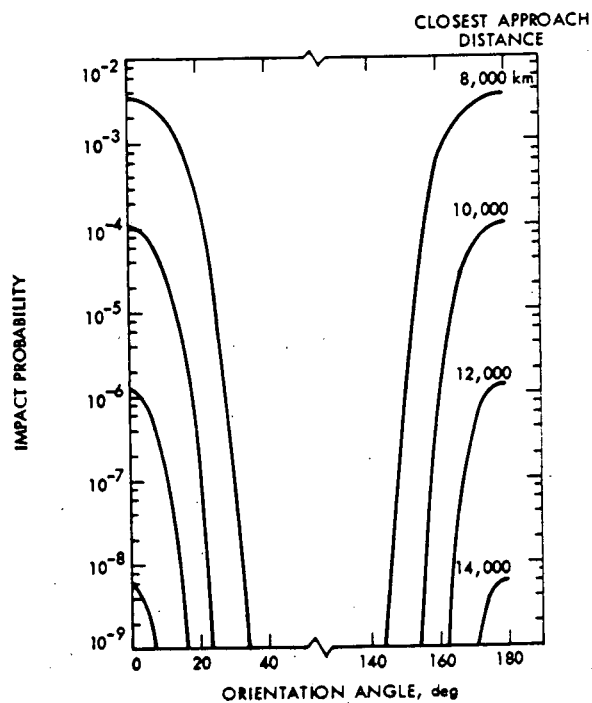


Fig. 1-A.5 Titan impact probabilities for various flyby designs, Maneuver 6

as would be expected with a circular error dispersion. However, in the case of maneuver 6, (shown in Fig. 1-A:5), the variation of impact probability with orientation angle is dramatic. The probability of impact can change from a value, which could lead to quarantine violation, to one which is nil, simply by changing the orientation of the aim point. There would be no change in the distance of the spacecraft from the satellite. This situation did not occur in the case of the analyses for the planets, Jupiter and Saturn.

1.1.3 Conclusions

The following summarizes the conclusions:

- 1) Midcourse connection maneuvers, occurring during the Jupiter-Saturn leg, are critical in terms of possible quarantine violations at Titan.
- 2) Satellite quarantine has implications on flyby geometry, in that the probability of impact may be a function of orientation of the aim point relative to the impact area.
- 3) Strategies for satisfying satellite quarantine should be correlated with those used to satisfy planetary quarantine.

The significant result of the analyses described is that the probability of impacting a satellite due to a midcourse correction maneuver, can be a function of the orientation of the aim point relative to the satellite impact area, for a constant distance of closest approach. This is important because the orientation of the aim point will probably be selected on the basis of the scientific return expected. Therefore, it is recommended that mission planners correlate their selection of an aim point with members of the quarantine community.

1.1.4 Problem Areas

The main problem encountered was a lack of software to do the analyses. Such software was developed during the task.

1.1.5 Future Activities

- 1) The probability of impact analyses described here will be applied to encounters of Tethys (Saturn) and Ganymede and Io (Jupiter).
- 2) The analyses were performed for a satellite encounter preceding the planetary encounter. The analyses will be repeated for a post planet encounter and the results compared with those described here.
- 3) The implications of a JS - X mission (optional encounter) on satisfying quarantine constraints will be investigated.
- 4) Fuel load penalties resulting from the satisfying of quarantine constraints (where $P_I > 6.4 \times 10^{-5}$) will be determined; and the use of navigation strategies to minimize them will be investigated.
- 5) The existence of interrelations between satisfying satellite and planet quarantine will be investigated.

1.1.6 Presentations

C. Gonzalez, "Strategies for Satellite Encounter, " presented at the Semiannual NASA Sterilization Technology Seminar, New Orleans, Louisiana, January 30-31, 1973.

1.2 JUPITER ENTRY ANALYSIS

1.2.1 Subtask B Introduction

The objective of the Jupiter atmospheric entry analysis subtask is to develop and use the tools needed to determine the thermal response characteristics of a typical spacecraft and related debris upon entry into the Jovian atmosphere.

Since the entry heating received by a body entering Jupiter's atmosphere is appreciable (due to the inertial entry speed of 61 km/sec), it is appropriate to investigate the possible microbial burden reduction resulting from the temperature increase.

The problem has been broken down into determining the heat received in the two primary aerodynamic regimes of the atmosphere, the free molecular and the continuum.

The entering body first encounters the free molecular regime which is the more rarified portion of the atmosphere. The energy transfer to the body results from exchanges of kinetic energy; similarly to the transfer of energy between colliding billiard balls. Thus, it is much simpler to calculate the temperature increase (both because of the energy transfer mechanism and because of lower heat loads) here than when the body enters the denser continuum regime.

1.2.2 Significant Accomplishments

The first phase of Subtask B involved the determination of temperature increases to selected spacecraft components and debris (including particles in 1 to 100 μm range) entering the upper regions of the planetary atmosphere from outer space (therefore, in the free molecular regions).

The selected components included:

- 1) Thermal blankets
- 2) Antenna
- 3) Supporting struts

These components were selected on the basis that their composition would make them the most susceptible to the heat loads encountered in the early entry.

Analyses were performed to determine the temperature increases for particles in the 1 to 1000 μm range as a function of particle size, material, specific gravity and entry angle for three atmospheric models*. Average values were assumed for emittance and accommodation coefficient. The emittance determines the amount of energy radiated away - high emittance leading to lower temperature. The accommodation coefficient relates to the

* Warm, nominal and cool models as described in the following reference:

NASA Space Vehicle Design Criteria Monograph, "The Planet Jupiter (1970)," NASA SP-8069, December, 1971.

heat absorbed by a body entering through the molecular regime, due to its collision with the molecules of the atmosphere. The accommodation coefficient depends both on the body surface material and the composition of the atmospheric gas.

Analyses have been completed for plastic particles using a value for the accommodation coefficient of 0.2 and thermal emittances of 0.15, 0.35 and 0.55. Plastic particles were chosen because this type of material could be produced during various types of disintegration processes and could contain viable organisms. The analyses will be extended in a parametric fashion in order to bound the problem with respect to values of accommodation coefficient and emittance. This is being done by using a closed form solution to the equations. Figure 1-B.1 shows an example of the type of result obtained for plastic particles. Particle size is plotted versus entry angle and the region of possible microbial survival is indicated. In this context the boundary for survival was taken to be an instantaneous temperature of 350°C.

The thermal response of multi layer thermal blankets in the free molecular regime was analysed for various entry angles ranging from 5° to 90° for the three atmospheric models. The thermal blanket was considered both in

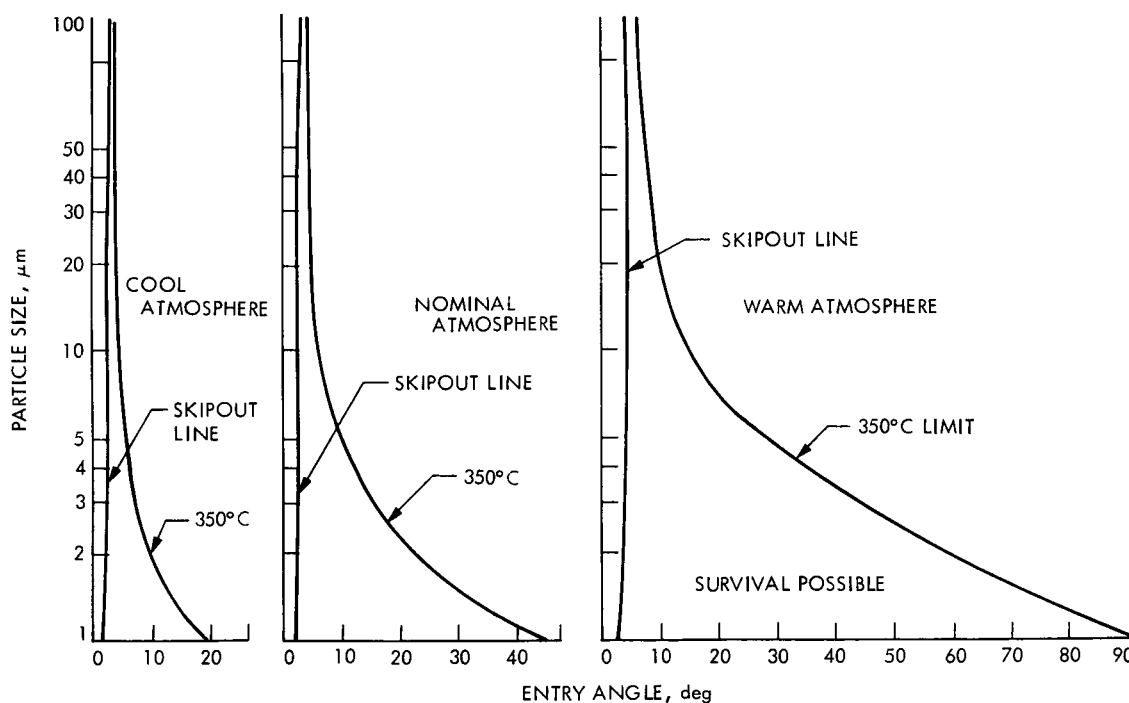


Fig. 1-B.1 Thermal corridors for plastic particles

steady and tumbling entries. The blanket consists of an outer layer of teflon aluminized on one side and inner layers of mylar aluminized on both sides.

Tests performed on samples indicated that melting and disintegration took place at temperatures of 400°C. These disintegration processes would also yield a multitude of flakes which, if produced in flight, may disperse and proceed individually along their own entry path.

The analyses indicated that motion at reasonable small angles of inclination with tumbling provided the best chance for microbes surviving entry. The overall analyses showed that the possibilities ranged from ablation of all layers to cases where a good number of layers remained intact. A significant finding was that due to the very high resistance of the heat flow, interior layers remained at ambient temperature while disintegration occurred in the outer layers. Therefore, "cold" ejecta could be produced containing viable particulates. Figure 1-B.2 provides an example of the results obtained.

Thermal response analyses for the antenna were performed for two directions of motion - frontal and edge on. This type of analysis bounds all possible intermediate cases including tumbling. The antenna is an aluminum honeycomb structure whose thin facing is approximately 0.3 mm thick. Figure

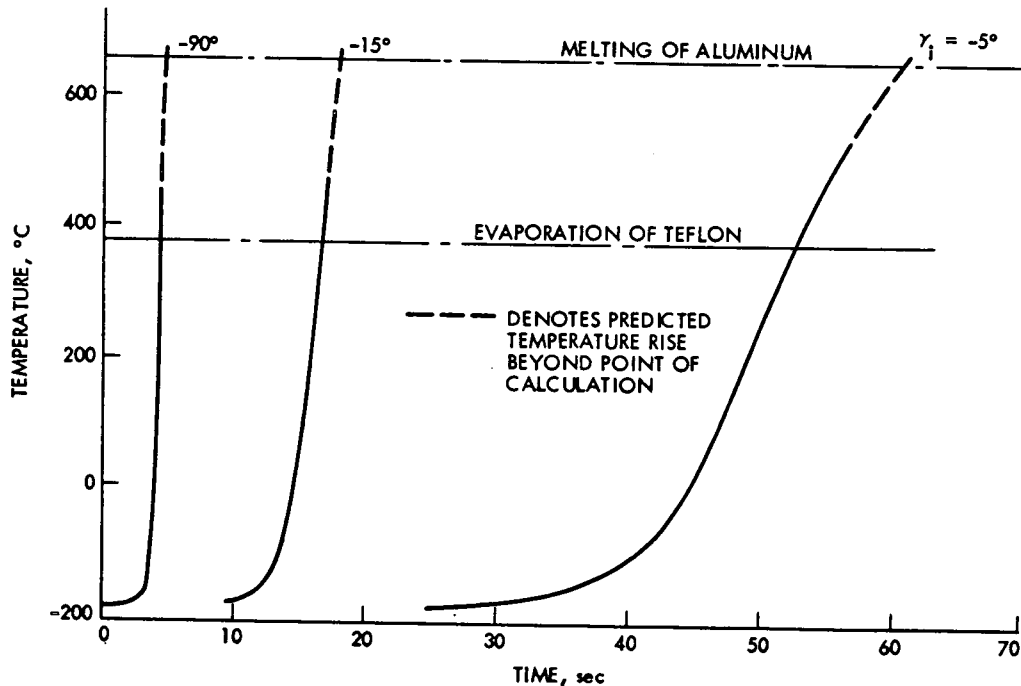


Fig. 1-B.2 Typical thermal response of blankets, outer planets spacecraft -- nominal atmosphere

1-B.3 is a schematic of the antenna structure. Frontal motion would be in the direction of the Z-axis and edge on in the direction of the Y-axis. The structure is broken down into nodes or slices for the purpose of thermal analysis.

Figure 1-B.4 shows the results obtained for the frontal motion case. Decomposition is reached at the front in all cases. Decomposition was not reached at the back side at the time of termination of the calculation.

Figure 1-B.5 is a graphic representation of the edge on case. Only nodes 1 through 8 and 281 through 288 are plotted, i.e., the section of highest temperature profile and the section adjacent to X-X plane. All other profiles, above X-X plane, will show a progressive downward displacement.

Due to a very low thermal conductance, the temperature drop across the graphite epoxy face sheet is very rapid both at the front and back sides. Moreover, the temperatures along Y-Y plane of upper portion of the antenna and, of course, at some angular distance away from this plane, have substantially exceeded a decomposition temperature of the front graphite epoxy sheet in the case of the cool atmosphere. Both have resulted in decomposition of graphite epoxy and melting of aluminum in the case of the warm atmosphere. Obviously, decomposition and disintegration have begun before the times for which these maximum temperature profiles, shown in Figure 1-B.5 were reached.

Results of tests involving the heating of a sample of graphite epoxy show that graphite epoxy completely outgasses at 650°C , and also delaminates to the extent that the individual graphite fibers for most part are only loosely held together. This was confirmed by looking at a heated sample through a microscope. When handled (after cooling) sample would easily break up in thin strips and fibers. Thus, a complete self separation into fibers may take place at a temperature somewhat higher than 650°C .

The bonding of the graphite epoxy sheets (or strips as the case may be) to the aluminum honeycomb is done by epoxy resin. Normally this bond becomes destroyed when structure temperature exceeds the bond decomposition limit ($250\text{-}300^{\circ}\text{C}$). At such time the face sheet and honeycomb structure will separate. This separation, depending on the conditions of flight, may be partial with respect to total surface of the antenna or complete.

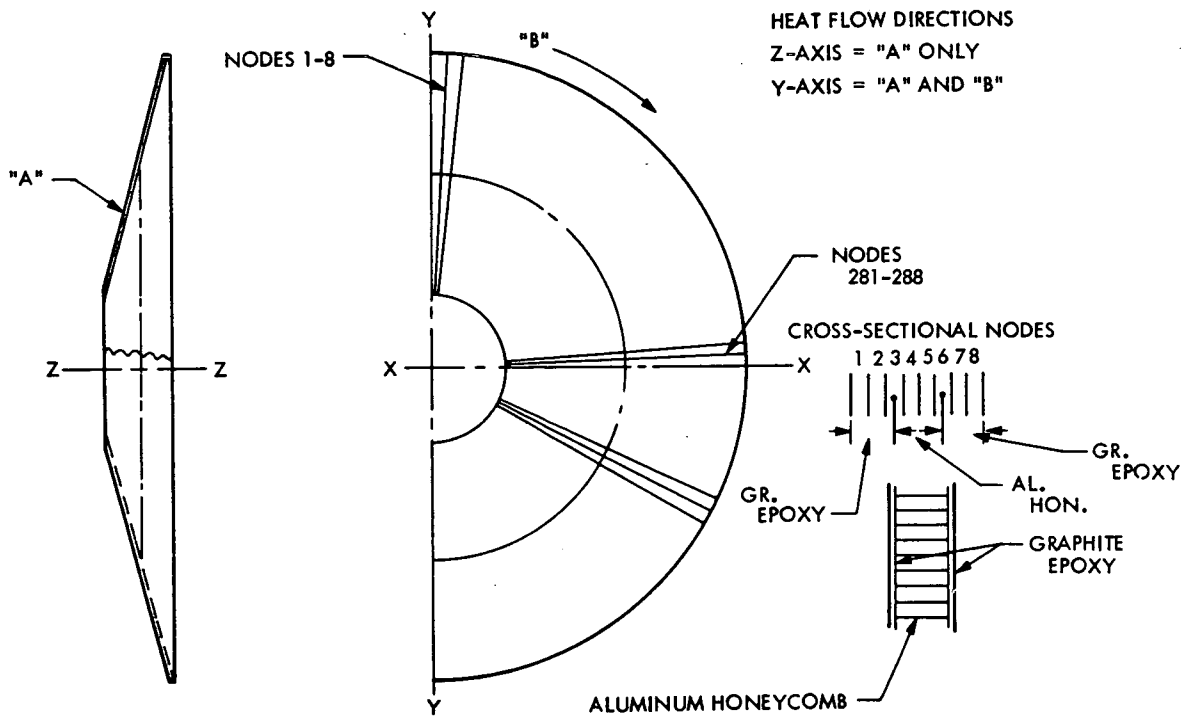


Fig. 1-B.3 Antenna geometry

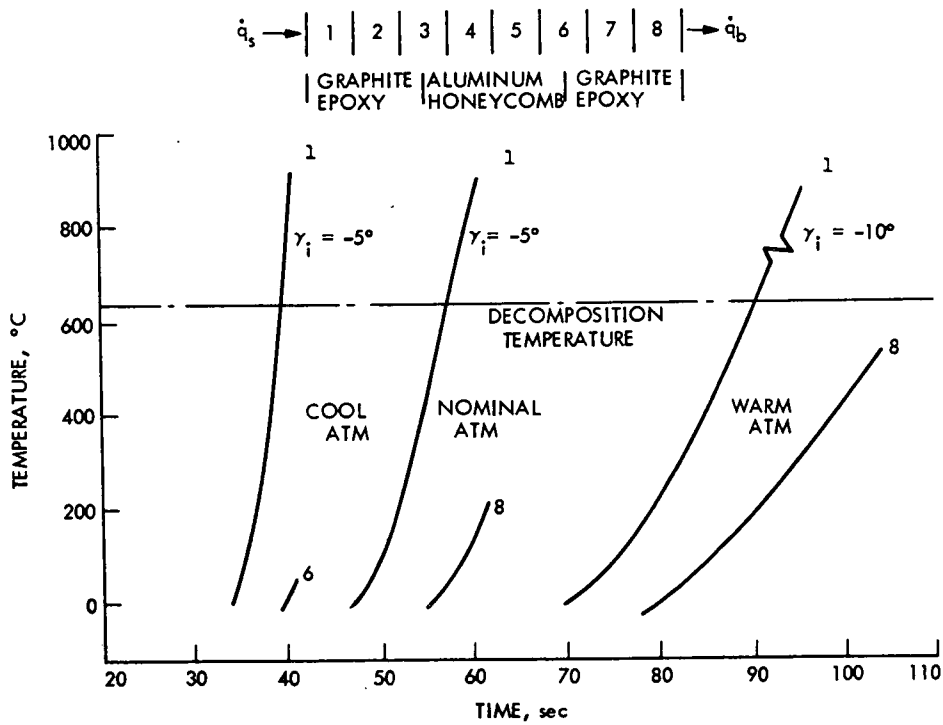


Fig. 1-B.4 Antenna temperatures at continuum flow boundary, face orientation - non ablating structure

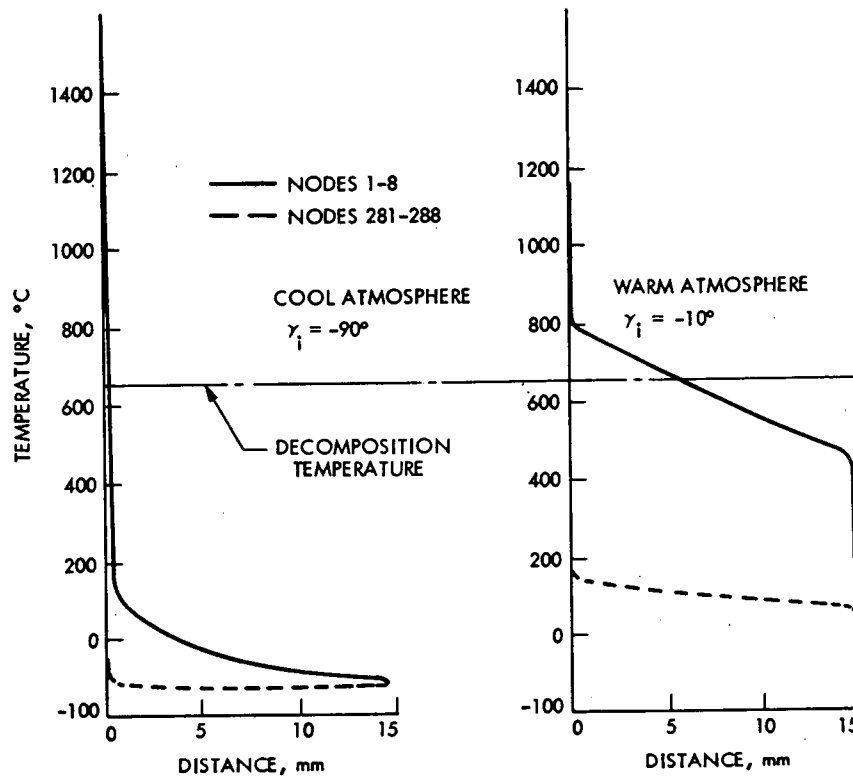


Fig. 1-B.5 Antenna temperatures at entry into continuum, edge orientation -- non ablating structure

With the spacecraft tumbling, the heating of the antenna takes place on both sides in a cyclic manner. Judging by the two cases examined (Z-axis and Y-Y plane), and in view of the very low thermal conductance across the antenna face sheet, the surface temperature will be very high, in parts, causing the type of disintegration described above. In addition, the centrifugal force due to rotation may disperse some of the pieces of graphite epoxy already disintegrated due to heating.

In summary, the antenna will at least be partially disintegrated before reaching the continuum flow. It should be borne in mind that since the heating rate increases with time as the entry into the continuum flow begins, the protruding support strut ends, unshielded either by the bus or the disintegrating antenna, will melt away separating the antenna from the bus. This conclusion can be reached on the evidence presented in para. 1.2.2.1. The separated antenna,

whether in steady or tumbling motion, continues to heat and disintegrate rapidly. Once the thin graphite epoxy layer has eroded on one side, the same high heating rate will be impressed instantly on the aluminum honeycomb and graphite epoxy layer on the back side. The latter is due to large voids (open space) in the honeycomb structure. In only a very short time, tumbling antenna temperatures (on both sides) become comparable in magnitude to those generated on one side during a steady motion. However, due to irregular heating pattern, small particles loosely attached to the structure may still be set free without being adequately heated.

The following summarizes the status of the spacecraft as it enters the continuum flow regime.

1.2.2.1 Supporting Struts. These are assumed to be made of thin wall aluminum tubing. The data generated indicate that the approximate strut temperatures for representative entries were as follows:

Warm atmosphere, entry at $\gamma_i = -10^\circ$		689°C (just above melting)
	-45°	80°C
	-90°	110°C
Nominal atmosphere	-5°	395°C
	-45°	-80°C
	-90°	-65°C
Cool atmosphere	-5°	145°C
	-45°	-95°C
	-90°	-82°C

The above temperatures should be considered as reasonably the lowest to be expected.

Inspection of the continuum flow convective entry heating rates (available from entry trajectories data) indicates that initially these rates could vary from 0.4 to 0.8 kw/cm² for the warm atmosphere and between 1 to 3 kw/cm² for the nominal and cool atmospheres. Assuming conservatively the net rates to be only 0.1 kw/cm² for the warm and 0.5 kw/cm² for the nominal and cool atmospheres, the calculated temperature increase rates in the aluminum struts become approximately 2000° K/s and 1000° K/s, respectively. The calculated time to reach the melting temperature of aluminum (~650°C) was on

average 0.55s in the warm atmosphere and 0.037s in the nominal or cool atmospheres. These times constitute approximately 1 to 1 1/2% of continuum flow total entry time, and for all practical purposes the melting away of the struts should be regarded as almost instantaneous.

The maximum stagnation pressure associated with the strut disintegration was different in each entry case, but it was never higher than a good fraction of 1 kN/m^2 (less than 0.01 atmosphere). Thus, a conclusion is reached that a collapse of strut structure is caused primarily by heat.

1.2.2.2 Metal Appendages. On the basis of the above evaluation it is possible to conclude that all metal and strutlike, uninsulated, and exposed (to flow) appendages will meet similar fate, i. e., they will be melted away very quickly on entry into the continuum flow.

1.2.2.3 Radioisotope Generators. It is believed that this assembly by itself could be regarded as inherently sterile and, as such, will be eliminated from the present study. This is because the internal temperature of the unit is approximately 1100°C , and the outside skin approximately 300°C at all times. Separate evaluation is made when any sort of blanket wrapping is present (due to heat exchange devices etc.).

1.2.2.4 Science Platform. The platform will be immediately separated from the spacecraft because of collapse of the strut structure. The same applies to the other science experiments, such as energetic particle instrument, plasma probe, and meteoroid impact and optical detectors. It is expected that only the platform complement of instruments, taken together as one assembly, needs investigating, and that the results will be applicable to the rest of science experiments mounted separately.

1.2.2.5 Bus Assembly. This assembly, left by itself, includes the propulsion engine, propellant and gas tanks, and the canopus tracker, in addition to the bus structure and electronic and power equipment normally housed in the bus bays. Blanket coverage is assumed of the front and rear of the bus. As found earlier in this study, the blankets will be in the state of disintegration.

1.2.2.6 Summary. Figure 1-B.6 provides a stage-by-stage view of spacecraft illustrating its disintegration process. The sketch is a representation of the spacecraft status described above, and is self-explanatory.

In addition to the analyses involving the free molecular regime, the continuum calculations (cold wall convective and radiative heating) were repeated for entry trajectories at orbital speed. They were performed for the three atmospheric models, values of ballistic coefficient of 0.5, 5, 50, and 500 kg/m² and of nose radii from 0.001 to 0.3 m. Only shallow entry angles were considered (10, 3, 1 deg), since this kind of entry is seen as an end to multiple skip-out.

In general, the results indicate that the radiative flux present for the larger nose radii in hyperbolic entry (non-orbital case) has vanished, except for a small contribution coming in at the largest radius and heaviest body. The convective heating, and thus the total heating, is appreciably less than for the corresponding hyperbolic entry. Other features of interest are:

- 1) The rise in heating for the very shallow 1 deg entry is quite marked, due to the longer entry time.
- 2) The warm atmosphere case has high heating due to the increased gentle gradient of density with height, i. e., longer time to decelerate.

1.2.3 Conclusions

The thermal blanket and antenna would undergo either partial or full disintegration depending on the atmospheric model and angle entry used. As the thermal blanket and antenna disintegrated, they would release debris composed both of manufactured materials and contaminants introduced during manufacturing.

Components not destroyed in the upper regions would, during entry conditions, be totally destroyed as the components and release of debris is made on entry and continues deeper into the atmosphere (continuum).

The struts would melt shortly after entry of the spacecraft into the continuum, causing the spacecraft to traverse the rest of the way as separate pieces.

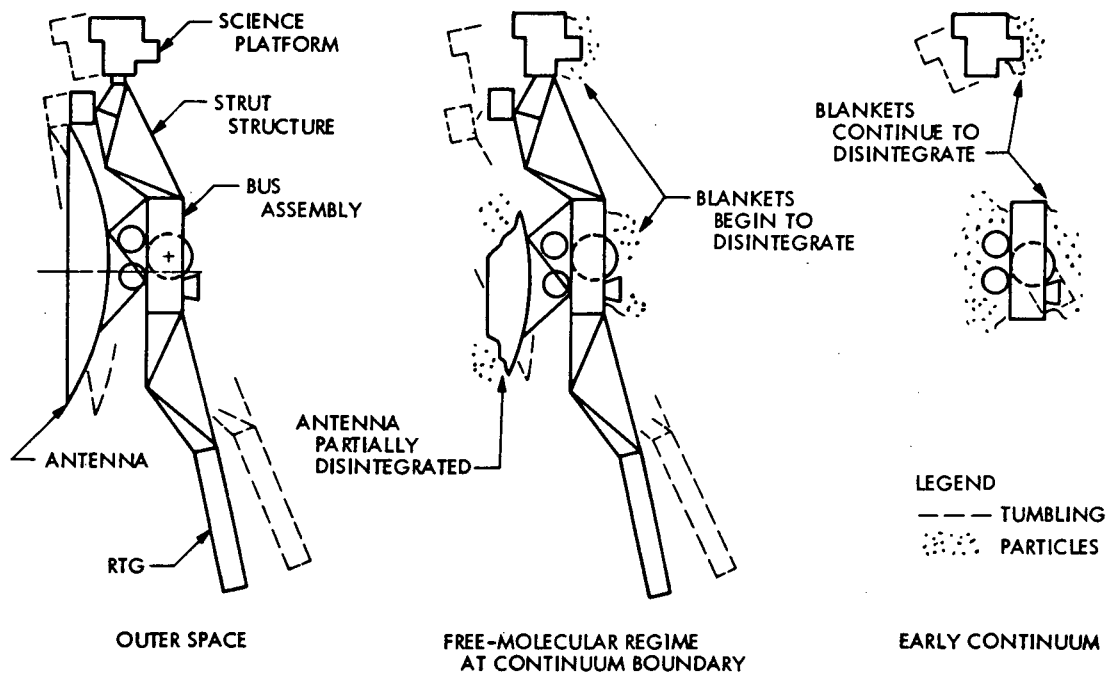


Fig. 1-B.6 Disintegration stages of outer planets spacecraft

The results of calculations on small particles (1 - 100 μm) indicate that some may survive the heat pulse and reach a terminal velocity. It remains to be determined if these small particles could become suspended in biologically interesting zones of the atmosphere.

These results would have to be modified and extrapolated to determine the fate of the debris released upon disintegration of components, such as the thermal blanket and antenna. Although large components would be in the continuum regime where heat loads are greater, particles, by virtue of their size, would still experience free molecular regime conditions.

1.2.4 Meaning of Results to Planetary Quarantine

The results indicate that only those organisms ejected during the disintegration of a major component would stand any chance of survival. Those organisms which continue to reside within the component would be destroyed before they reached the atmospheric zone with greatest potential for growth.

1.2.5 Future Activities

The following future activities will be completed based on a reallocation of resources for the task:

- 1) Completion of the analyses for small particles including:
 - a) Maximum temperature calculations based on closed form parametric solutions.
 - b) Determination of ambient atmospheric densities and temperatures where small particles reach subsonic and terminal flight.
 - c) The bounds on the thermal emittance and accommodation coefficient for establishing survivability of organisms.

These analyses will cover all particulates, including those released during disintegration.

- 2) Thermal response analysis of a cylindrical plastic lens cover as it traverses the continuum regime. This is performed in lieu of analyses on larger components necessitated by a reallocation of funds.
- 3) Interpretation of the meaning of the results obtained in terms of probable survival of organisms.

1.2.6 Presentations

W. Jaworski, "Jupiter Entry Analysis" presented at the semiannual NASA Sterilization Technology Seminar, New Orleans, Louisiana, January 30-31, 1973.

SECTION II

NATURAL SPACE ENVIRONMENT STUDIES (NASA No. 193-58-61-02)

<u>Contents</u>	<u>Title and Related Personnel</u>
Subtask A para. 2.1	<p>EFFECT OF PLANETARY TRAPPED RADIATION BELT ON MICROORGANISMS</p> <p>Cognizance: D. Taylor</p> <p>Associate Personnel: C. Hagen (Bionetics) J. Barengoltz C. Smith (Bionetics) G. Renninger (Bionetics)</p>
Subtask B para. 2.2	<p>EFFECT OF SOLAR WIND ON MICRO-ORGANISMS</p> <p>Cognizance: D. Taylor</p> <p>Associate Personnel: C. Hagen (Bionetics) J. Barengoltz</p>
Subtask C para. 2.3	<p>EFFECT OF SPACE VACUUM ON MICROORGANISMS</p> <p>Cognizance: D. Taylor</p> <p>Associate Personnel: C. Hagen (Bionetics) R. Gildersleeve (Bionetics) G. Simko (Bionetics) J. Yelinek (Bionetics) C. Smith (Bionetics)</p>
Subtask D para. 2.4	<p>PROBABILITY OF GROWTH IN PLANETARY ATMOSPHERES AND SATELLITES</p> <p>Cognizance: R. Berkman</p> <p>Associate Personnel: D. Taylor G. Gonzalez C. Hagen (Bionetics) T. Divine F. Palluconi</p>

2.1 EFFECT OF PLANETARY TRAPPED RADIATION BELT ON MICROORGANISMS

2.1.1 Subtask A Introduction

The objective of this subtask is to determine the effect of planetary trapped radiation belts on the survival of microorganisms associated with a nonsterile spacecraft.

With flyby missions now planned for Jupiter and Saturn and possible Jupiter orbiters and probes, the trapped radiation belts may represent an environment lethal to microorganisms; thus reducing the requirement for decontamination of spacecraft before launch.

The major components of planetary trapped radiation belts are electrons and protons. The approach of the present task is to evaluate possible biological effects of these belts by subjecting spacecraft microbial isolates to different energies, exposures and dose rates of these particles.

2.1.2 Significant Accomplishments

During this reporting period a spacecraft bacterial subpopulation (nine sporeforming and three nonsporeforming isolates) plus two comparative organisms, Staphylococcus epidermidis and Bacillus subtilis var. niger, were exposed to 2 MeV protons at different exposures and exposure rates with simultaneous exposure to a vacuum of 10^{-6} torr at 20 and -20 C.

A preliminary analysis of the data indicates that approximately 23, 16 and 6% of the initial populations survived fluences of 5×10^{11} , 1×10^{12} , and 5×10^{12} protons cm^{-2} , respectively. B. subtilis was found to be less resistant than most of the sporeforming spacecraft isolates. The nonsporeforming isolates were generally more sensitive to the same levels of radiation.

The isolates were found to be more sensitive to fluxes (exposure rate) of 10^8 and 10^9 protons $\text{cm}^{-2} \text{ sec}^{-1}$ than to a flux of 4×10^{10} protons $\text{cm}^{-2} \text{ sec}^{-1}$.

2.1.3 Future Activities

Future activities in this subtask area will involve investigation of the effect of higher energy protons on spacecraft microbial isolates. Studies will

be initiated to evaluate the effect of electrons of the less than 2 MeV class. In addition, studies will be made of the amounts and types of secondary radiation resulting from interaction of primary radiation with the spacecraft surfaces.

2.2 EFFECT OF SOLAR WIND RADIATION ON MICROORGANISMS

2.2.1 Subtask B Introduction

The objective of this subtask is to determine the effect of solar wind radiation on microorganisms associated with nonsterile spacecraft.

This study is directed towards determining the reduction in spacecraft associated microbial burden attributable to solar wind radiation.

The approach does not attempt a simulation of the total radiation environment, but rather to examine the effect of low energy electrons and protons as a function of dose and energy. The data acquired would apply to all missions.

2.2.2 Significant Accomplishments

During this reporting period, a work statement was initiated for an RFP to study the overall effect of solar wind radiation on spacecraft microbial isolates. The contractual study will include determining the effect of three energies, exposures and dose rates of low energy electrons and protons.

2.2.3 Future Activities

Future activities in this task area will involve selection of a contractor.

2.3 EFFECT OF SPACE VACUUM ON MICROORGANISMS

2.3.1 Subtask C Introduction

This study was designed to examine the combined effects of space vacuum and spacecraft temperatures on the survival of microorganisms. Fourteen isolates were exposed to the test conditions. Nine of the isolates, recovered from MM'71 spacecraft, were sporeformers while three isolates were nonsporeformers. A sporeforming organism, Bacillus subtilis var. niger, and a non-sporeforming organism, Staphylococcus epidermidis ATCC 17917, were included in the tests for comparative purposes.

A vacuum exposure (10^{-8} torr) of the bacterial isolates to temperatures of -40, 25, 40, and 55°C were conducted for 7, 14, 28, 56, and 187 days to simulate the vacuum and temperature environment of a spacecraft during a typical mission to Mars.

2.3.2 Significant Accomplishments

2.3.2.1 Experimental Conditions.

Microbiology. The test organisms, isolated from MM'71 spacecraft, are the same organisms that were used in the launch pressure profile study and are presently being used in the space radiation study. The derivation, culture, and assay procedures for the isolates are described in para. 3.2.1.2 of the Annual Report (JPL Doc. No. 900-597, February 1973).

Vacuum Equipment. Photographs, together with a description of the test facility, are presented in para. 3.2.1.2 of the Annual Report (JPL Doc. No. 900-597, February, 1973).

2.3.2.2 Results. Additional studies were conducted during the report period to determine whether or not a vacuum exposure could activate dormant spores which, in turn, would result in viable spore recoveries of greater than 100 percent when compared to initial populations.

All scheduled vacuum temperature exposures have been completed. A statistical evaluation of the data is being conducted.

Spore Activation Studies. Three types of tests were conducted:

- 1) Heat shock of the spore suspensions at 80°C for 18 min;
- 2) Incubation of the spores in a solution of calcium dipicolinate; and
- 3) A one and 7 day(s) vacuum exposure of the spores to 25°C.

Based upon initial tests, the calcium dipicolinate system* for activation of dormant spores without heat shock was effective in activating spores of only one of the isolates. For this reason further consideration of calcium dipicolinate as a spore activator was discontinued.

*Riemann and Ordal, (Science 133:1703-1704, 1961).

Table 2-C.1 shows the effect of heat shock and vacuum exposure on spore activation of the isolates. The numbers in the table are ratios of heat shocked (HS) to nonheat shocked (NHS) spores. Numbers greater than 1.00 indicate that heat shock or vacuum exposure activated the spores with a resultant higher viable cell count occurring after treatment. Numbers less than 1.00 indicate that the particular spores do not require heat or vacuum exposure for maximum recovery or that the spores are susceptible to either heat shock or vacuum exposure.

Table 2-C.1 Effect of vacuum at 25°C on spore activation

Isolate number	Test exposure, days		
	0	1	7
1	0.99*	0.92	1.07
2	1.01	1.07	1.08
8	1.97	0.92	1.73
9	1.14	0.93	1.04
11	2.82	5.03	1.66
12	2.53	2.15	0.95
13	0.95	1.03	1.00
16	1.12	0.69	0.97
18	2.70	0.97	2.68
BSN	0.99	0.56	0.98
*Expressed as the Ratio of Heat Shocked/Non Heat Shocked Viable Cell Counts			

Prior to vacuum exposure it was found that spores of isolates 8, 11, 12, and 18 required heat shock for maximum spore activation while spores of isolates 1, 2, 9, 13, 16, and B. subtilis var. niger did not require heat shock for maximum spore activation.

There was a variety of responses of the sporeforming isolates to the vacuum exposure. Spores of isolates 1, 2, 9, and 13 were not significantly affected by exposure to vacuum for 1 or 7 day(s) as indicated by no significant change in the HS/NHS ratios before exposure and after the 1 and 7 day(s) exposure.

A 1- or 7-day vacuum exposure could substitute for heat activation with spores of isolates 8, 12, and 18. With spores of isolate 8, a decrease in the HS/NHS ratio occurred after a 1-day vacuum exposure. This was followed by a return to dormancy of the spores during a 7-day vacuum exposure as shown by the subsequent rise in the HS/NHS ratio. The same pattern of spore activation after a 1-day vacuum exposure followed by a return to the dormant state after a 7-day vacuum exposure occurred with spores of isolate 18. Spores of isolate 12 showed increased activation only after the 7-day vacuum exposure.

Spores of isolate 11 exhibited an increased dormancy after the 1-day vacuum exposure as indicated by the large increase in the HS/NHS ratio. With an extended vacuum exposure of 7 days, the spores of isolate 11 became activated with a decrease in the HS/NHS ratio.

A possible heat sensitization of spores of isolates 16 and B. subtilis var. niger occurred after a 1-day vacuum exposure. The spores returned to their normal state of heat resistance during the 7-day vacuum exposure. This was evidenced by the HS/NHS ratio decreasing after 1-day vacuum exposure and the HS/NHS ratio increasing after 7 days to a value similar to the HS/NHS ratio before vacuum exposure.

Vacuum exposure as a substitute for spore activation should not be taken as an unusual phenomenon. The review article by Keynan and Evenchik* (Activation, pp. 358-396) cites numerous papers that deal with physical and chemical agents as spore activators.

*The Bacterial Spore. Edited by G. W. Gould and A. Hurst. Academic Press, New York, 1969.

Vacuum Temperature Studies. Since the data analyses are not complete, several sporeforming and nonsporeforming isolates were selected to demonstrate differences in resistance of the isolates to the test environment.

Figure 2-C.1 shows the vacuum temperature resistance of spores of two spacecraft isolates. The log numbers of spores, shown in Fig. 2-C.1 for each exposure time and temperature, is the geometric mean based upon four replicates with the 95% confidence limit shown as a vertical bar at each test point. For comparison purposes the vacuum temperature resistance of B. subtilis var. niger spores are included.

Spores of isolate 9, one of the more sensitive to the vacuum temperature environment, were affected by 40 and 55°C temperatures as early as 7 days. By 187 days spore viability of this isolate decreased also at 25°C. No viable spores were recovered after an 187-day vacuum exposure at 55°C.

Spores of isolate 1, one of the more resistant to the vacuum temperature environment, were not significantly affected by any of the temperatures during the initial 7 days of vacuum exposure. Spore viability decreased by 56 days after vacuum exposure to 55°C and after an 187-day vacuum exposure to 40 and 55°C.

Spores of the comparative organism, B. subtilis var. niger, resembled the resistance of spores of isolate 9. With B. subtilis var. niger, spore viability decreased after vacuum exposure to 25, 40, and 55°C during the initial 7 days. However, after 56 days spore viability had only decreased after vacuum exposure to 55°C. The nonsignificance of 25 and 40°C on spore viability after the 56-day vacuum exposure may be related to the reversible state of spore dormancy-activation. After 187 days spore viability decreased from vacuum exposure to 25 and 40°C and no viable cells exposed to 55°C were recovered.

Cell viabilities of selected nonsporeforming spacecraft isolates and the comparative organism, S. epidermidis, after exposures to the vacuum temperature environment for 7, 56, and 187 days are shown in Fig. 2-C.2. The log numbers of bacteria, shown in Fig. 2-C.2 for each time and temperature, is the geometric mean based upon four replicates with the 95% confidence limit shown as a vertical bar at each test point.

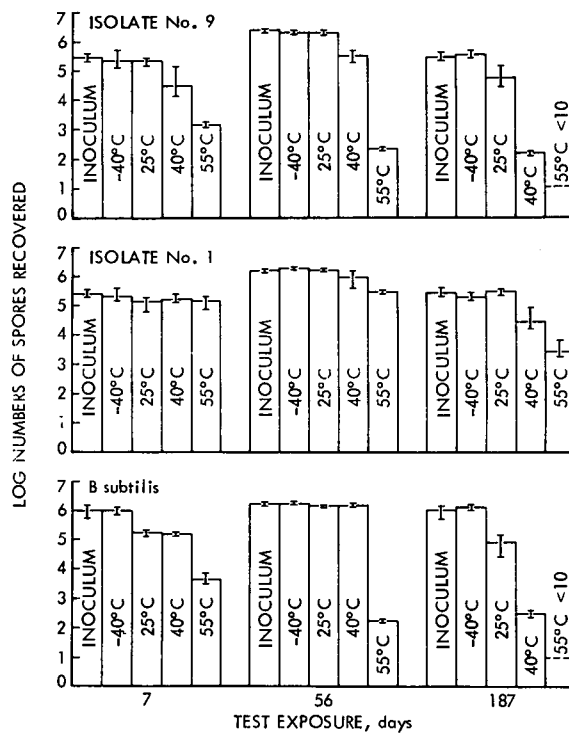


Fig. 2-C.1 Vacuum temperature resistance of spores of spacecraft isolates

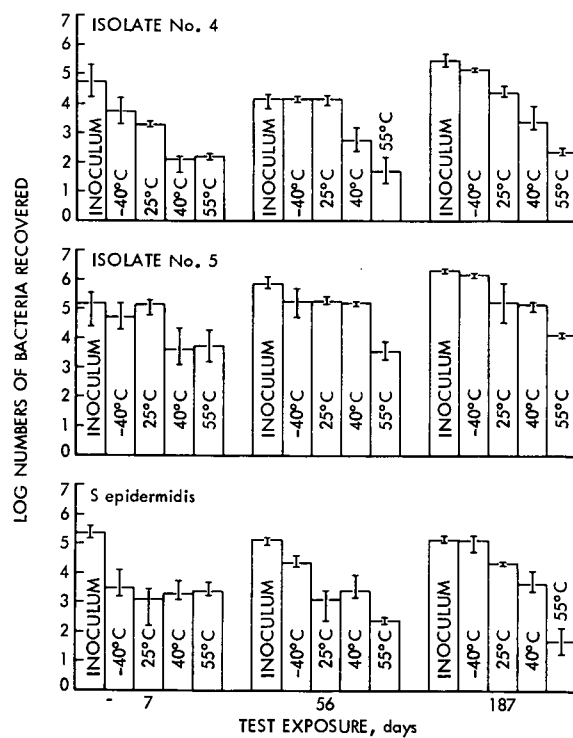


Fig. 2-C.2 Vacuum temperature resistance of nonsporeforming spacecraft isolates

Isolate 4 cell viability decreased after a 7, 56, and 187-day vacuum exposure to 40 and 55°C. A vacuum exposure at 25°C for 7 and 187 days, but not 56 days, also significantly decreased cell viability. The no apparent effect of 25°C after a 56-day vacuum exposure may be related to cell clumping or other unknown factor(s).

The cell viability of isolate 5 decreased after a 7, 56, and 187-day vacuum exposure to 40 and 55°C and after a 56 and 187-day vacuum exposure to 25°C.

The results from tests with S. epidermidis, although somewhat erratic, indicated that cell viability was significantly decreased after a 7, 56, and 187-day vacuum exposure to 25, 40 and 55°C.

In general, vacuum exposure to -40°C did not have a great effect on cell viability even after an 187-day vacuum exposure. It also appeared that cell viabilities of the nonsporeforming spacecraft isolates were similar to, or better than, the cell viabilities of spores of spacecraft isolates. This was particularly true with vacuum exposures to 55°C.

Table 2-C.2 presents the approximate log reductions of both spores of sporeforming isolates and vegetative cells of nonsporeforming isolates after vacuum exposure to -40, 25, 40, and 55°C for 56 and 187 days.

Selection of the 56 and 187-day vacuum exposures was based upon a mission time similar to the 1971 Mariner to Mars (MM'71). Temperature recordings of the MM'71 mission indicated that by 56 days the majority of the spacecraft's exposed surface will be less than 40°C. It is acknowledged that the time-temperature relationship may not hold true for other Mars missions because the possible trajectories are dependent upon the relative positions of Earth and Mars.

In general, however, there was very little effect of -40 and 25°C after either a 56- or 187-day vacuum exposure on cell viability. A temperature of 55°C for 56 days and temperatures of 40 and 55°C for 187 days significantly reduced the cell viability.

After a 56-day vacuum exposure to 40 and 55°C spore viability was reduced approximately 0.6 and 2.0 log(s), respectively, and the nonsporeforming

Table 2-C.2 Log reduction of spacecraft isolates

<div> <div>Tempera- ture</div> <div>Isolate No.</div> </div>	Test exposure, days							
	56				187			
	-40	25	40	55	-40	25	40	55
<u>Spores</u>								
1	*	0.0	0.5	0.8	0.4	0.0	1.0	2.0
2	0.5	0.2	0.3	2.0	0.0	0.4	1.6	4.0
8	0.0	0.0	*	0.5	0.0	1.0	1.4	2.7
9	0.2	0.2	1.0	4.0	0.0	0.8	3.6	>5
11	0.6	0.1	0.1	0.7	0.6	0.6	0.9	>4
12	0.2	0.5	0.3	1.1	*	0.0	0.3	2.3
13	0.3	0.7	0.8	1.8	0.2	0.8	1.5	>5
16	0.6	0.1	0.3	1.4	*	0.3	0.7	2.6
18	*	*	0.0	2.1	*	*	1.1	>5
BSN	0.0	0.5	0.4	4.0	0.0	1.1	3.5	>6
<u>Vegetative</u>								
4	0.0	0.0	1.5	2.5	0.6	1.1	2.2	3.1
5	0.7	0.7	0.8	2.4	0.6	1.4	1.5	2.7
19	0.6	0.7	0.8	3.0	0.4	0.8	1.6	2.0
SE	0.7	2.1	1.7	2.7	0.2	0.8	1.6	3.6
* >100% survival								

isolate viability was reduced 1.0 and 2.6 log(s) after a vacuum exposure to these same respective temperatures.

After an 187-day vacuum exposure to -40 and 25°C the spore viability was reduced approximately 0.1 and 0.5 log, respectively, while the nonspore-forming isolate viability was reduced 0.5 and 1.1 log(s) after a vacuum exposure to these same respective temperatures.

Certain summary statements, based upon results to date, can be made:

- 1) The effect of space vacuum in conjunction with normal operating temperatures of spacecraft on the survival of spacecraft isolates was found to be highly dependent upon the duration of exposure, temperature, and the individual isolates;
- 2) Temperatures of -40 and 25°C did not effectively reduce initial populations even after an 187-day exposure; and
- 3) Temperatures of 40 and 55°C, while effective in reducing initial populations, did permit survival after as long as an 187-day exposure.

2.3.3 Problem Areas

The problem, as stated in previous reports, has been resolved. This problem dealt with greater viable cell recoveries after exposure to the vacuum temperature environment than were initially present. Demonstration has shown that vacuum exposure, or the events leading to vacuum exposure, can activate dormant spores that may initially require heat shock for maximum spore activation.

2.3.4 Future Activities

Future activities of the vacuum temperature study will deal with completion of the data analyses and preparation of the final report.

2.3.5 Presentations

Hagen, C.A., "Effect of Space Vacuum on Microorganisms," presented at the semiannual NASA Spacecraft Sterilization Technology Seminar, New Orleans, Louisiana, January 30-31, 1973.

2.4 PROBABILITY OF GROWTH IN PLANETARY ATMOSPHERES AND SATELLITES

2.4.1 Subtask D Introduction

In a previous study (para. 2.4.6, Ref. 1), zones of high and low probability of growth were defined for the atmosphere of Jupiter. Since Jupiter lacks a solid surface, organisms would probably have to be suspended in the troposphere, presumably by wind currents, in order for growth to occur. The high probability of growth for this region, extending from about 10 to 100 Earth atmospheres of pressure, is based on an analysis of temperature, chemical composition, including availability of water, carbon and nitrogen sources, suitable pH, and the absence of inhibitory factors such as excessive radiation. To relate all of these factors to probability of growth, each of the minimal growth requirements for microorganisms was considered with respect to its availability on Jupiter.

In the present report, results are described of an analysis of pH and water in the high probability of growth region of Jupiter. The report identifies the high probability of growth regions for the planet Saturn and presents an analysis of probability of growth for the satellites of both Jupiter and Saturn.

2.4.2 Significant Accomplishments

2.4.2.1 Review of Microbial Growth Requirements. Previous reports have described the environmental extremes of temperature, pressure and chemicals tolerable by growing bacteria (para. 2.4.6, Ref. 2), and the minimal values of moisture and nutrients which still allow growth (para. 2.4.6, Ref. 1). In general, bacteria require a source of carbon and nitrogen for synthesizing structural components and for energy to carry on metabolic processes. These bacteria also require a variety of inorganic salts and water. If any one of these components is lacking, growth (according to the "law of limiting factors"), cannot occur. This law is also employed in defining zones where probability of growth is high, low, or nil.

2.4.2.2 Water and pH in the Jupiter Atmosphere. The previously defined high probability region for Jupiter (para. 2.4.6, Ref. 1) was reported to have a pH between 11 and 12. A more extensive pH analysis has been completed, based on water and abundance of NH_3 , pressure, and temperature. The most important factor affecting pH is the solubility of ammonia in water which is greatly influenced by temperature.

The cool atmospheric model predicts the presence of liquid water in the high probability of growth region of Jupiter. The average relative humidity, is only about 5 percent ($A_w = 0.05$) in the suitable temperature regions for all models, considerably lower than minimal A_w levels at which bacterial growth has been observed (para. 2.4.6, Ref. 2). However, the troposphere is a region of changing weather conditions, including regular occurrences of rain (cool model). Thus, growth could occur intermittently, if not continuously, in this region.

Figure 2-D.1 shows the theoretical pH profile for Jupiter model atmospheres as a function of temperature. The vertical lines indicate where growth is possible in the temperature range. The two points indicate theoretical pH values for temperatures of -50° and 0°C . These values are approximately pH 14.0 and 12.5, respectively. At locations below the water and ammonia clouds the relative abundances of these constituents can only be estimated. Linearity was assumed in extrapolating to these deeper atmospheric regions (dotted line) such that at a temperature near 100°C , one might expect a pH of about 10.5. Again, the values shown are based on calculations of average abundances and do not take into consideration the effects of rains or other factors which could alter these values.

2.4.2.3 Probability of Growth in the Saturn Atmosphere. Because of the greater distance of Saturn from the Earth, data obtained for Saturn are less reliable than those for Jupiter. Saturn, like Jupiter, does not possess a solid surface (para. 2.4.6, Ref. 3). Owing to its considerably greater distance from the Sun, temperatures for Saturn are proportionately lower than those for Jupiter. Nevertheless, an internally generated heat source provides a region in which temperatures are suitable for microbial growth. Pressures in this region are higher than pressures found in the analogous temperature zone identified for Jupiter. The higher pressures imply greater abundances of all

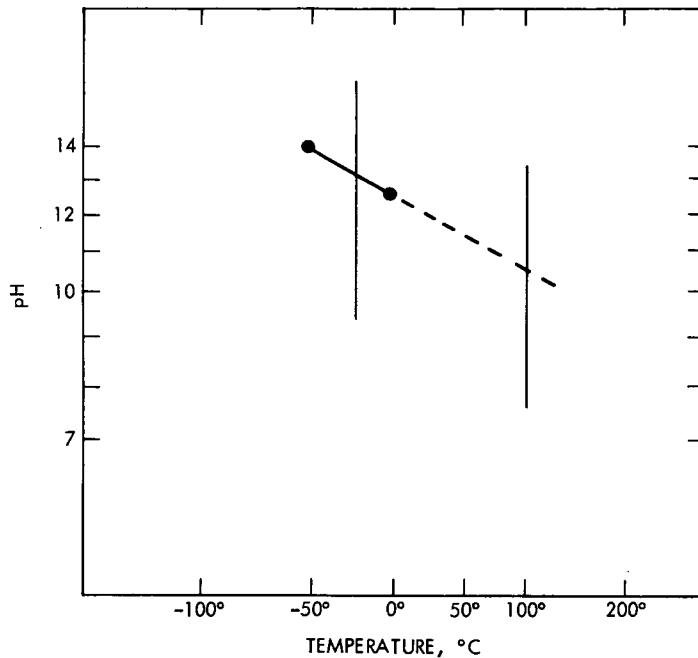
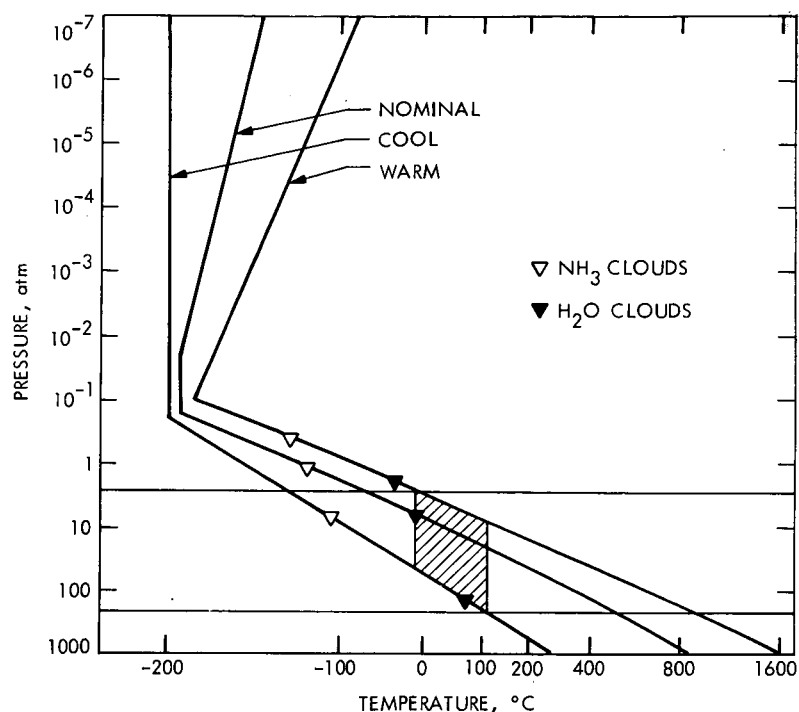


Fig. 2-D.1 pH values vs temperature in highest P_g regions of Jupiter model atmospheres

chemical constituents. In addition, based on atmospheric analyses, liquid water should be present in the nominal model as well as in the cool model predicted for Saturn. The cool and warm models of both Jupiter and Saturn represent the extreme cases predicted for these environments. Since, for Jupiter liquid water is predicted only for the cool model, probability of growth can be expected to be higher for Saturn than for Jupiter. Figure 2-D. 2 indicates the temperature and pressure relationships for the Saturn atmosphere, showing the warm and cool extremes as well as a nominal curve. The cross-hatched area indicates the region where microbial growth could be possible. Additionally, the open and closed triangles indicate the locations of NH_3 and H_2O clouds, respectively. The two horizontal lines of Fig. 2-D. 2 confine the pressure regions to a range of about 3 to 200 Earth atmospheres.

2.4.2.4 Probability of Growth on Satellites of Jupiter and Saturn. The satellites of Jupiter and Saturn are referred to as the "icy satellites" because of their chemical composition. While empirical measurements are relatively few, Lewis (para. 2.4.6, Ref. 4) has calculated the chemical composition of the icy satellites on the basis of solar chemical abundances, condensation properties of



From NASA Document "NASA SP-8091", June 1972

Fig. 2-D.2 Pressure vs temperature for the Saturn model atmospheres

the elements, and temperatures at the time of accretion. Table 2-D.1 summarizes the calculated average chemical composition of the icy satellites.

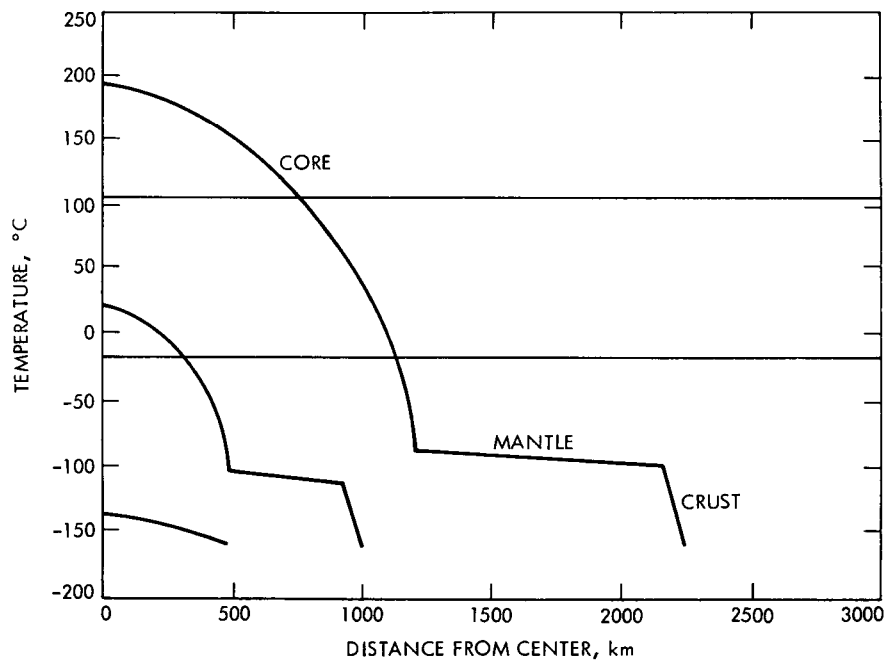
While Table 2-D.1 lists the major chemical components of these satellites, there is the likelihood that other compounds required for growth (e.g., phosphorus compounds and various divalent cations) are present at least in trace amounts. Presently, however, there are no means available to detect traces of such compounds.

While all growth promoting compounds may be present on the satellites, these compounds may be absent in regions where growth could occur. During accretion, for example, certain essential elements could have migrated to the satellite core, a region of poor accessibility.

Surface temperatures of the icy satellites are generally very low, probably averaging around -150°C . Surface temperatures are basically independent of size, but could be greatly affected by the presence of an atmosphere (para. 2.4.6, Ref. 5). Figure 2-D.3 describes the theoretical temperature

Table 2-D.1 Chemical components of icy satellites

Species	Approximate weight, %
H ₂ O	54
FeO	15
SiO ₂	13
NH ₃	10
MgO	8
(CH ₄)	(<5)



From: Icarus 15, 174-185 (1971). J. S. Lewis "Satellites of the Outer Planets: Their Physical and Chemical Nature"

Fig. 2-D.3 Temperature profiles of icy satellites
(No Atmosphere)

profiles of satellites of radii 500, 1000 and 2250 km, assuming the absence of an atmosphere. The large satellites are composed of three distinct regions, a relatively thin crust, a "slushy" mantle and, presumably, a mudlike core. The horizontal lines of Fig. 2-D. 3 indicate a temperature region suitable for growth only in the cores of the larger satellites. The cores of large icy satellites are presumably still warm as the result of radioactive decay occurring several billion years ago and, as indicated in the figure, assuming a mantle having great insulating properties (para. 2.4.6, Ref. 4). It can also be seen that satellites of 500 km radius or less are probably cold and undifferentiated.

Table 2-D. 2 describes significant properties of the four largest Jupiter satellites and Titan, a satellite of Saturn. Satellites smaller than these have probability of growth values approaching nil, because of their complete lack of atmosphere and extreme cold. The primary importance of atmospheres is not in the provision of growth constituents; but rather in the retention of heat that would otherwise be lost. This means that for satellites having relatively dense atmospheres, such as Titan, the temperature profiles (Fig. 2-D. 3) could require significant modification. Relatively thin crusts might thus be thinner than postulated, thin enough to allow penetration of microorganisms or release of richer materials from below. However, it should be noted (Table 2-D. 2) that atmospheres of the Gallilean satellites are rather sparse, both in water vapor and other gases.

The conclusions drawn from Table 2-D. 2 and Fig. 2-D. 3 are that the four Jupiter satellites Io, Europa, Ganymede, and Callisto, while having traces of atmosphere, have surface temperatures which are probably too low to allow growth of microorganisms. There is some possibility, however, that growth could occur on localized regions of the Gallilean satellites if the surfaces were differentiated. Differentiation could include surface areas having cracks and crevices from which rich materials from the mantle or core erupt in a manner somewhat analogous to volcanic or geyser activity. For Titan the abundant atmosphere most certainly indicates surface temperatures much higher than the theoretical - 180°C.

2.4.2.5 Relative Ranking of Probability of Growth for Jupiter, Saturn and their Satellites. Absolute probability of growth values cannot be calculated reliably for the planetary bodies discussed here. On the basis of current knowledge, a

Table 2-D.2 Significant properties of satellites considered in the P_g analysis

	Radius, km	Density, g/cm ³	Possible Constituents	Atmosphere		Water Vapor Pressure, N/m ²
				Surface Pressure, N/m ²	Surface Tempera- ture, °C	
<u>Jupiter</u>						
Io	1800	2.8	CH ₄ , NH ₃	<0.01	-109	<10 ⁻³
Europa	1550	3.0	CH ₄ , NH ₃	<0.01	-108	<10 ⁻³
Ganymede	2800	1.7	CH ₄ , NH ₃	<0.01	-106	<10 ⁻³
Callisto	2500	1.5	CH ₄ , NH ₃	<0.01	-105	<10 ⁻³
<u>Saturn</u>						
Titan	2400	2.3	CH ₄ , NH ₃ H ₂ , He	>150	>>-180	Saturation

relative rank ranging from high to nil probability of growth can be assigned to each body. Such a ranking is shown in Fig. 2-D.4. Saturn has been assigned the highest probability of growth in the likelihood that liquid water and relatively high concentrations of nutrients are available. Jupiter has a somewhat lower probability of growth because there is only a 10 to 20 percent chance that water is present as a liquid. Titan has been ranked high on the basis of its atmosphere and the accompanying greenhouse effect. The actual surface temperature of Titan cannot be ascertained at this time because radiation measurements probably provide data on the upper atmosphere only. Hence, the ranking for Titan is tentative. The four Gallilean satellites of Jupiter have been ranked considerably lower than Titan, and can be considered to have a low probability of growth. Smaller satellites including the rings of Saturn, which are probably composed of icelike rocks up to a few km in diameter, have essentially a nil probability of growth.

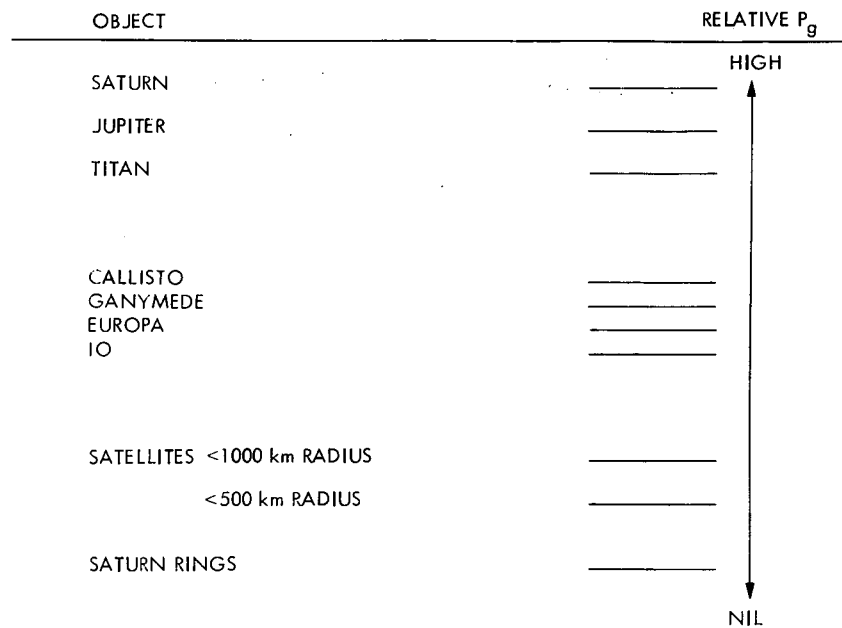


Fig. 2-D.4 Relative probabilities of growth for Jupiter, Saturn and their satellites

2.4.3 Relevance to Planetary Quarantine

An entry analysis (see JUPITER ENTRY ANALYSIS, Section I, para. 1.2) has indicated that spacecraft directed at Jupiter or Saturn will have disintegrated partially before reaching the high probability of growth regions. Breakup of the spacecraft could result in sterilization of released organisms. Whether released organisms maintained their viability during entry into a high probability of growth region was not considered in the present task.

Regarding a possible satellite encounter, only one satellite, namely Titan, appears to have a relatively high probability of growth risk. This conclusion is based on limited data showing that Titan has a relatively dense atmosphere. The four Galilean satellites were found to be of little probability of growth concern; but, as has been discussed, there is a finite probability of growth identified for these larger bodies. It has also been indicated that in regard to probability of growth smaller satellites will not be of concern to future space missions.

2.4.4 Future Activities

A refinement of the present probability of growth analysis will require, in part, the accumulation of new data on the planets and satellites. When new data are obtained, e. g., by use of space probes and more sophisticated measuring devices, and when experiments are completed on growth of microorganisms in simulated space environments, it should be possible to provide a more reliable analysis of several of the planetary bodies discussed here. Specifically, additional data would be useful in defining the physical and chemical composition of the Jupiter and Saturn atmospheres with more certainty, and in measuring surface characteristics of the satellites. Of particular interest would be an analysis of the lower atmosphere and surface of Titan.

2.4.5 Presentation

Berkman, R. M., "Probability of Growth in Jovian Planetary Atmospheres and Satellites," presented at the NASA Semiannual Sterilization Technology Seminar, New Orleans, Louisiana, January, 1973.

2.4.6 References

1. Planetary Quarantine Annual Review, Space Technology and Research, July 1971 - July 1972, February 1973.
2. JPL Document 900-556, Planetary Quarantine Semiannual Review, Space Research and Technology, January 1 - June 1971.
3. NASA SP-8091, The Planet Saturn (1970), June 1972.
4. Lewis, J. S., "Satellites of the Outer Planets: Their Physical and Chemical Nature," ICARUS 15, pp. 174-185, 1971.
5. Hunter, D. M., "The Atmosphere of Titan," Comments on Astrophysics and Space Physics, 4, pp. 149-154, 1972.

SECTION III

POST LAUNCH RECONTAMINATION STUDIES
(NASA No. 193-58-62-03)

<u>Contents</u>	<u>Title and Related Personnel</u>
Subtask A para. 3.1	Cognizance: J. Barengoltz Associate Personnel: J. Yang C. Bauerle (Bionetics) R. Gildersleeve (Bionetics)

3.1 POST LAUNCH RECONTAMINATION STUDIES

3.1.1 Subtask A Introduction

The objective of this task is the development of an analytical technique for the evaluation of the probability of the relocation of particles from nonsterile to sterile areas on a spacecraft.

The recontamination process is important for all multiple missions with separate microbiological burden allocations for the various mission phases, and critical for life detection experiments that risk contamination from non-sterile components.

The approach has been to study the effects of typical mission environments on the distribution of particles on spacecraft surfaces both analytically and experimentally.

3.1.2 Significant Accomplishments

During this reporting period, the effort has been devoted to the spacecraft phase, where the important environments for particle release are pyro events and meteoroid impacts. Computer codes to calculate previously developed new analytical solutions and simpler solutions for meteoroid impact have been in development. In the particle release experiment, the in vacuo glass bead phase has been completed and the data are being analyzed. Plans for improved test procedures and follow-on experiments are being formulated. The last area is the grain (particle) trajectory analysis, where the critical quantities are the electric field and grain charge. Analyses and computer codes for the electric field at and near an illuminated plate in the solar wind plasma and the charging rates and equilibrium potential for particles have been completed. There is also a preliminary trajectory code for the particles.

3.1.3 Future Activities

Future activities will involve integrating of the three dimensional electric field and final trajectory routine with the geometry code. Operational meteoroid impact codes will be completed, and particle release experiments will be performed with more realistic samples.

SECTION IV
SPACECRAFT CLEANING AND DECONTAMINATION
TECHNIQUES
(NASA No. 193-58-67-02)

<u>Contents</u>	<u>Title and Related Personnel</u>
Subtask A para. 4.1	PHYSICAL REMOVAL OF SPACECRAFT MICROBIAL BURDEN Cognizance: H. Schneider Associate Personnel: R. Gildersleeve (Bionetics)
Subtask B para. 4.2	VERIFICATION OF USSR HYDROGEN PEROXIDE DECONTAMINATION AREA Cognizance: M. D. Wardle Associate Personnel: G. Renninger (Bionetics)
Subtask C para. 4.3	EVALUATION OF PLASMA CLEANING AND DECONTAMINATION TECHNIQUES Cognizance: D. M. Taylor Associate Personnel: R. Olson (Boeing)

4.1 PHYSICAL REMOVAL OF SPACECRAFT MICROBIAL BURDEN

4.1.1 Subtask A Introduction

Present planetary quarantine constraints for flyby and orbiter vehicles require maintaining the microbial burden on the spacecraft below a certain critical level. State-of-the-art clean room facilities and contamination control techniques do not assure that this critical level can be maintained throughout necessary assembly and test operations.

A system was developed to physically detach and remove particulates from surfaces by means of individual jets expanding from a stationary or fluctuating pressure source in combination with low vacuum flow such as that produced by commercial vacuum cleaners.

4.1.2 Significant Accomplishments

A test apparatus to simulate steady state blow-vacuum cleaning in a measurable and repeatable manner has been designed and fabricated. The systems affecting detachment and removal can be independently controlled and allow for a separate study of the mechanics involved. The assembly of the apparatus and its installation in a 100 x microscope has been completed. Initial calibration and pilot tests will commence next month.

4.1.3 Future Activities

Future activities will involve investigation into the effectiveness of pulse flow and vectored high energy sonic waves.

4.2 VERIFICATION OF USSR HYDROGEN PEROXIDE DECONTAMINATION DATA

4.2.1 Subtask B Introduction

The primary objective of this subtask is to evaluate hydrogen peroxide as a bactericidal agent for use on spacecraft hardware. Relevant work in the USSR has indicated the practicality of such an application of hydrogen peroxide. The Russian work points to the sporicidal properties of hydrogen peroxide. At present the accepted decontaminant in the Mariner series has been isopropyl

alcohol (70%) which is generally recognized as nonsporicidal. It is the purpose of the present task to assess the merit of hydrogen peroxide decontamination of appropriate United States spacecraft.

4.2.2 Approach

A literature search was conducted to identify related work in the area. The most pertinent publications were found in the Russian literature. The information derived from these articles was then used in design of experimentation to assess the time-concentration effects of hydrogen peroxide on spacecraft isolates and representative microorganisms. The data from this study will be used for testing of application techniques to spacecraft hardware. This study will examine the bactericidal effects on both pure cultures and heterogeneous, naturally-occurring population representative of those found on spacecraft surfaces.

4.2.3 Significant Accomplishments

Survivor data were generated for 7 sporeformers and 3 nonsporeformers exposed to concentrations of 3, 10, and 15 percent hydrogen peroxide. Two comparative organisms were included; i. e., Staphylococcus epidermidis and spores of Bacillus subtilis var. niger. Challenge cultures of spores were suspended in 95% ETOH while those of nonsporeformers were water suspensions harvested from 48 hr culture plates. All challenge cultures were approximately 10^8 viable organisms/ml. The test procedure (Fig. 4-B.1) involved inoculation of 1 ml of challenge suspension into a flask containing 100 ml of 3, 10, or 15% H_2O_2 held in a water bath at 25°C. Following appropriate exposure, 1 ml aliquots were removed from the flask and placed in 9 ml of sterile catalase to dissipate H_2O_2 . After all H_2O_2 was dissipated (as determined by a $KI/FeSO_4$ test sensitive to 1 part H_2O_2 in 25 million) ten-fold serial dilutions were made in 1% peptone water and from these TSA pour plates formed. All tests were performed in triplicate. A $KMnO_4$ titration of test solutions of peroxide were performed at time₀ and time_t to verify H_2O_2 concentrations. Table 4-B.1 shows the effects of 3, 10, and 15% H_2O_2 on spores. As can be seen, some spore activation and isolate variability was observed; however, with moderate exposure times the peroxide showed pronounced sporicidal effects. The percent

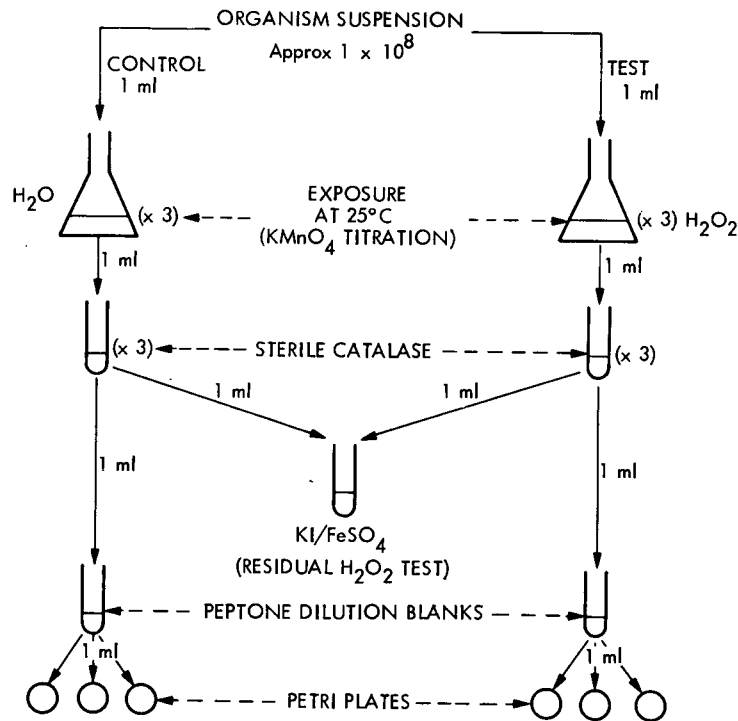


Fig. 4-B.1 Hydrogen peroxide test procedure

survival of vegetative cells exposed to hydrogen peroxide is shown in Table 4-B.2. No viable vegetative cells were recovered after a ten minute exposure time.

4.2.4 Future Activities

Future activities in this task area will entail an evaluation of application techniques for spacecraft surfaces.

4.2.5 Presentations

"Verification of USSR Hydrogen Peroxide Decontamination Data," presented at the NASA Semiannual Planetary Quarantine Technology Seminar, New Orleans, Louisiana, January, 1973.

Table 4-B.1 Percent survival of spores exposed to hydrogen peroxide

H ₂ O ₂ , %	Test Organism	Exposure Time, min.			
		2	30	60	150
3	BSN*	112.0	4.66	0.0064	0
	16	109.0	21.8	2.1	0
	1	97.5	57.9	0.71	0
	2	114.0	25.8	5.9	0
	13	121.6	129.0	44.3	0.3
	12	21.4	0.096	0.0022	0
	18	43.5	11.9	0.95	0
		$\bar{X}^{**} = 84.5$	$\bar{X} = 41.1$	$\bar{X} = 9.0$	$\bar{X} = 0.05$
10	BSN	102.0	0.012	0	0
	16	34.9	0.0024	0	0
	1	81.7	0	0	0
	2	111.0	0.11	0	0
	13	148.8	3.6	0	0
	12	2.0	0	0	0
	18	3.22	0	0	0
		$\bar{X} = 63.6$	$\bar{X} = 0.62$	$\bar{X} = 0$	$\bar{X} = 0$
15	BSN	69.5	0.012	0	0
	16	22.0	0.0022	0	0
	1	67.1	0	0	0
	2	100.7	0	0	0
	13	139.2	0	0	0
	12	0.065	0	0	0
	18	0.63	0	0	0
		$\bar{X} = 54.9$	$\bar{X} = 0.0004$	$\bar{X} = 0$	$\bar{X} = 0$

*Bacillus subtilis var. niger
 **Mean of spacecraft isolates.

Table 4-B.2 Percent survival of vegetative cells exposed to hydrogen peroxide

Isolate	Hydrogen Peroxide, %					
	3		10		15	
	Exposure		Exposure		Exposure	
	2 min	10 min	2 min	10 min	2 min	10 min
4	28	0	0	0	0	0
5	2	0	0	0	0	0
SE*	63	0	0	0	0	0

*Staphylococcus epidermidis

4.3 EVALUATION OF PLASMA CLEANING AND DECONTAMINATION TECHNIQUES

4.3.1 Subtask C Introduction

Heat and chemicals have been traditionally used as spacecraft microbial decontaminants. However, certain materials and complex equipment often suffer degradation and a loss in reliability due to heat damage or chemical incompatibility.

Plasma cleaning and sterilization involves exciting a gas and passing it over the material to be sterilized. The apparatus used includes a gas exciter (radio frequency), sterilization chamber and vacuum pump. In operation, specimens are placed in the sterilization chamber, pressure reduced, and excited gas is introduced. Sterilization is believed to occur although the parameters are not well understood, particularly as they may be applied to typical spacecraft applications. The plasma process does not appear to degrade materials which have been tested to date and, in addition, does not raise the temperature of the object being sterilized.

4.3.2 Significant Accomplishments

A contract proposal, compatible with the completed feasibility study, was evaluated. The contractual effort will provide the development of plasma sterilization technology for spacecraft application and generate preliminary design data for sterilizers. Specifically, this study will involve the lethality of different gases, penetration, design criteria, and material compatibility. The study will consist of two phases:

- 1) Define or determine the effective sterilizing ranges for different gases as a function of power and pressure
- 2) Determine penetration characteristics and material compatibility of plasma and develop design criteria for plasma sterilizers.

4.3.3 Future Activities

Future activities in this task area will involve an investigation into plasma decontamination techniques in terms of lethality of different gases, penetration characteristics, material compatibility, and sterilizer design criteria.

4.3.4 Presentation

"Evaluation of Plasma Cleaning and Decontamination Techniques," presented at the NASA Spacecraft Sterilization Technology Seminar, New Orleans, Louisiana, January, 1973.

SECTION V

PROBABILITY ESTIMATION METHODS AND ANALYSIS
(NASA No. 193-58-63-04)

Contents

Subtask A
para. 5.1

Title and Related Personnel

PROBABILITY ESTIMATION METHODS AND
ANALYSIS

Cognizance: A. Hoffman

Associate
Personnel: J. Yang

5.1 SUBTASK A INTRODUCTION

The objective of this task is to develop mathematical tools and methods for estimation of probability parameters for determining the probability of contaminating a planet with viable terrestrial organisms. This effort is intended to provide a link between the experimenter and the spacecraft planetary quarantine engineer for the development of probability of contamination values. Analytical techniques were formulated and used to transform experimental data into minimum and maximum probability estimates. The first undertaking was to critique the analytical approaches used for determination of planetary quarantine parameters and probabilities. The second was to develop an approach for microbial burden prediction. The third was to develop an analytical approach for analyzing the vacuum temperature data. The fourth was to formulate planetary quarantine standards in a theoretical manner and optimize the sterilization strategy. All of these efforts were completed during the reporting period. The results are discussed in the following paragraphs. The task conclusions are given in paragraph 5.3 (p. 5-19).

5.2 SIGNIFICANT ACCOMPLISHMENTS

5.2.1 Critique of Analytical Approaches Used for Determination of Planetary Quarantine Parameters and Probabilities

This effort is intended to:

- 1) Clarify the systematical approach for planetary contamination probability estimation
- 2) Criticize some of the approaches available in literature
- 3) Identify, within the systematical approach, what has not been done.

A schematic profile of the environments that microorganisms on a spacecraft would experience for a landed mission is given in Fig. 5-A. 1.

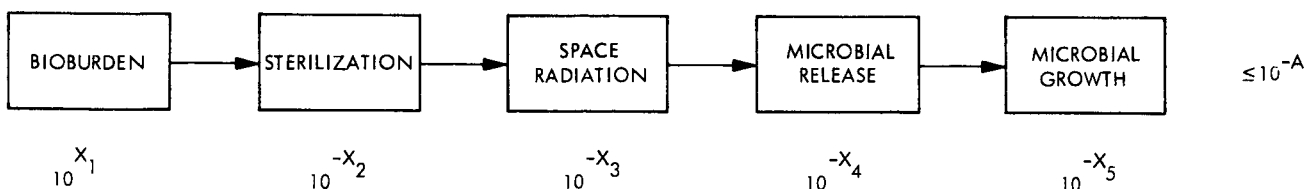


Fig. 5-A. 1 Schematic representation of contamination probability equation

5.2.1.1 Contamination Probability. According to the profile in Fig. 5-A.1, the probability of contaminating a planet, denoted by 10^{-A} , is expressed in Section V, Ref. 1 as follows:

$$10^{X_1} \cdot 10^{-X_2} \cdot 10^{-X_3} \cdot 10^{-X_4} \cdot 10^{-X_5} \leq 10^{-A} \quad (1)$$

in which

$$\begin{aligned} 10^{X_1} &= \text{initial microbial population} \\ 10^{-X_2} &= \text{probability of survival under sterilization cycles} \\ 10^{-X_3} &= \text{probability of survival under space radiation} \\ 10^{-X_4} &= \text{probability of release on a planet due to material fracture,} \\ &\quad \text{resulting from landing impact or erosion} \\ 10^{-X_5} &= \text{probability of growth and proliferation} \end{aligned}$$

Assuming that X_1 , X_2 , through X_5 are normally distributed random variables, the distribution of 10^{-A} is log-normally distributed and the confidence level is obtained in Section V, Ref. 1.

Two criticisms are given in the following text.

The formulation given in Eq. (1) is not representative. In fact, the formulations should read as follows:

$$\sum_{j=1}^N 10^{X_{1j}} \cdot 10^{-X_{2j}} \cdot 10^{-X_{3j}} \cdot 10^{-X_{4j}} \cdot 10^{-X_{5j}} \leq 10^{-A} \quad (2)$$

where j represents the j^{th} location of the microbial burden on the spacecraft. According to the location classification, the microbial burden can generally be summarized into four major categories, 1) exterior surface burden, 2) interior surface burden, 3) mated surface burden and 4) buried burden.

The associated release mechanisms and probabilities are quite different for these four locations. The total contamination probability is the sum of the

probability of contamination of each location category. This will be discussed later in detail.

For the formulation of Eq. (2), the approach proposed in Section V, Ref. 1 for computing the confidence level of the contamination probability cannot be applied. This is because the sum of log-normal random variables is not log-normally distributed. An appropriate method for the evaluation of the confidence level of the contamination probability is the method of moments.

The second criticism is that the uncertainties associated with X_1 , X_2 , through X_5 are neither clearly stated nor clearly defined. The definition of uncertainties associated with X_2 through X_5 are not trivial. This fact can be illustrated by considering a simple example of the effect of sterilizing environment in the following:

In a conventional model, the reduction in the microbial burden can be written as

$$10^{-X_2} = 10^{-t/D} \quad (3)$$

where D is the microbial resistance to sterilization and t is the time of sterilization. According to the experimental results, D is associated with some statistical dispersion for each t and each particular microorganism. Since the microbial populations are not necessarily homogeneous in their thermal resistance, the D value is different for different microbial subpopulations. In addition, there are also uncertainties associated with the estimation of D value from finite number of samples. Therefore, the uncertainties associated with D are quite complicated and require considerable effort to determine a reasonable approach for estimating this variability (e.g., the dispersion associated with D , to be used in Eq. (1)). For other events, such as fracture or erosion release probability, the problem becomes even more complicated. Therefore, it is proposed that effort be made toward clearly stating and defining the uncertainties, since it is a fundamental problem in the estimation of the final contamination probability. In this connection the approach of Bayesian statistics may be appropriate.

5.2.1.2 Bioburden Estimation. The estimation of bioburden existing on the spacecraft before sterilization has been attempted by many persons. The work by Roark (Section V, Ref. 2) has been critically examined. In general, the physical model established by Roark is reasonable. His solution is, however, too complicated for practical computation and for a sensitivity study to determine the correlation of critical parameters to the sample data. In addition, because of the complicated nature of the solution, one does not have an insight into the statistical distribution of bioburden.

The physical model is based on the following three assumptions:

- 1) Microorganisms exist in clumps on particles and the number of microorganisms in a clump is a random variable.
- 2) There exists a deposition mechanism due to fallout and contact, with a deposition rate $\lambda(t)$.
- 3) There exists a particle removal mechanism due to physical removal or death. The removal rate $\mu(t) N(t)$ is proportional to the number of viable particles existing on the surface at that time instant.

Assumption 1) takes into account the effect of clumping of viable microorganisms, while assumption 3) enables the model to reach a stationary solution called "plateau" effect, since the removal rate is proportional to the population of microorganisms.

With the physical model stated above, the population process $X(t)$, representing the number of microorganisms at time t , is a Markov process. Hence, the equation corresponding to the Kolomogorov forward equation for the transition probability can be derived (Eq. (9), Section V, Ref. 2). The derivation of Eq. (9) is unnecessary since it is very difficult to solve the equation. In fact, the author uses another approach to obtain the solution from Eq. (9), i. e., birth and death processes, for the solution of bioburden distribution.

Using the standard approach of the birth and death process (e. g., Section V, Ref. 3), the solution is easily obtained in Ref. 3, Eqs. 13-15. Ref. 3 Eqs. 13-15 involves the solution of the differential equation and a complicated

summation and factorial operation. Hence, the solution does not give a clear picture of the statistical distribution of bioburden.

Finally, the author did not obtain the stationary solution, i. e., the plateau state. If one considers the particle deposition and removal process as a nonhomogeneous Poisson process, then, the process of microorganism deposition and removal is a filtered nonhomogeneous Poisson process. The steady state solution can be obtained easily. In addition, the filtered Poisson process has a desirable property of asymptotical normality (Section V, Ref. 7). In other words, the statistical distribution of bioburden is asymptotically normal.

An approach based on the generation of system moments is given in para. 5.2.2.

5.2.1.3 Microbial Release Probabilities due to Material Fracture and Erosion.

The microbial release probabilities resulting from material fracture and erosion have been investigated, in some of its aspects, in Section V, Ref. 4. The formulation of this subject is important to the understanding and the identification of what has, and has not, been done in this area. Since the problem is not clearly formulated in Ref. 4, it is necessary to reformulate the problem in the following:

1. Microbial release due to material fracture. The fracture of spacecraft materials is assumed to be attributed to the landing impact. The extent of fracture is directly related to the impact velocity v which is a random variable.

Let $f(v)$ be the statistical distribution of landing velocity and let V^* be the velocity under which no fracture of materials occurs, called soft landing. Therefore, the probability of soft landing $P(s)$ is written as

$$P(s) = \int_0^{V^*} f(v) dv \quad (4)$$

The formulation can be given as follows:

$$\begin{aligned}
 \frac{P_c}{P(g)} = & M_{SX} \cdot P_{SX}(r|s) \cdot P(s) + M_{SI} \cdot P_{SI}(r|s) \cdot P(s) + M_m \cdot P_m(r|s) \cdot P(s) \\
 & + M_b \cdot P_b(r|s) \cdot P(s) + M_{SX} \cdot \int_{V^*}^{\infty} P_{SX}(r|v) f(v) dv \\
 & + M_{SI} \int_{V^*}^{\infty} P_{SI}(r|v) f(v) dv + M_m \int_{V^*}^{\infty} P_m(r|v) f(v) dv \\
 & + M_b \int_{V^*}^{\infty} P_b(r|v) f(v) dv
 \end{aligned} \tag{5}$$

where

P_c = probability of contaminating the planet resulting from materials fracture

$P(g)$ = probability that the microorganism will grow

M = microbial burden before landing

$P(r|s)$ = probability of release given a soft landing

$P(r|v)$ = probability of release given a high velocity impact landing with impact velocity v

Subscripts denote:

SX = exterior surface

SI = interior surface

m = mated surface

b = buried sources

The following assumptions can reasonably be made.

- 1) The probability of soft landing is very close to unity, i. e., $P(s) \approx 1.0$.
- 2) The probability of release $P_{SX}(r|v)$, $P_{SX}(r|s)$ of microorganisms on the exterior surface is 1.0. This is a conservative assumption.
- 3) Soft landing does not result in material fracture. This implies that $P_{SI}(r|s) = 0$, $P_m(r|s) = 0$, $P_b(r|s) = 0$, since for the microorganism on the interior surface, mated surface or buried in the materials, to be released, material fracture is needed.

Therefore, the formulation can be written as:

$$\begin{aligned} \frac{P_c}{P(g)} &= M_{SX} + M_{SI} \int_{V^*}^{\infty} P_{SI}(r|v) f(v) dv + M_m \int_{V^*}^{\infty} P_m(r|v) f(v) dv \\ &+ M_b \int_{V^*}^{\infty} P_b(r|v) f(v) dv \end{aligned} \quad (6)$$

Section V, Ref. 4 investigated the quantity $P_b(r|v)$ only, i. e., the probability of release of a buried microorganism given an impact velocity v .

Other quantities appearing in the above equation, which have not been investigated in the literature and are worthy of investigation, are listed in the following:

- | | |
|---------------|---|
| M_{SI} | = microbial burden on the interior surface before landing |
| M_m | = microbial burden on the mated surface before landing |
| M_b | = microbial burden buried in the materials before landing |
| $P_{SI}(r v)$ | = probability of releasing a microorganism on the interior surface under a high speed impact velocity v . This is equivalent to the probability of fracture of the protective materials resulting from high speed impact. |
| $P_m(r v)$ | = probability of release of microbes on the mated surface |

The microbial burden distribution on the exterior surface has been investigated by investigators, e.g., Roark (Section V, Ref. 2).

From the experimental data, $P_b(r|v)$ has been modeled in Ref. 4 by assuming that the probability of having a buried microorganism is uniformly distributed over the material volume,

$$P_b(r|v) = f(v) \cdot g(v) \cdot \lambda$$

where

$f(v)$ = fracture ratio

$g(v)$ = probability that a buried microorganism survives the fracture process

λ = depth coefficient

are all determined by the experimental results. The functional form for $f(v) \cdot g(v)$ was proposed (Section V, Ref. 4) as follows:

$$f(v) \cdot g(v) = \bar{f}_a \left[1 - e^{-\tau_f(v-V^*)} \right] \quad (7)$$

where \bar{f}_a and τ_f are constants to be determined by the experimental results.

The function given above for $f(v) g(v)$ is a monotonically increasing function of velocity v and it approaches \bar{f}_a asymptotically as $v \rightarrow \infty$. This functional form, however, contradicts the physical reasoning. It is realized that although the fracture ratio $f(v)$ increases as the velocity v increases, the survival probability of a microorganism decreases rapidly as the impact velocity v increases and hence, $f(v) g(v)$ should approach zero as $v \rightarrow \infty$. Hence, it is expected that the functional form of $f(v) g(v)$ should be such that it increases as v increases to a point and then decreases as v increases. A possible function with such functional characteristics is proposed in the following:

$$f(v) \cdot g(v) = \bar{f}_a \left[e^{-\tau_1(v-V^*)} - e^{-\tau_2(v-V^*)} \right] \quad (8)$$

where \bar{f}_a , τ_1 and τ_2 are parameters determined to fit the experimental data. Such a function, in fact, satisfies the experimental results (Section V, Ref. 5).

It is further realized that the function $f(v) g(v)$ is highly dependent on 1) spacecraft materials, 2) ground characteristics of landing site, such as rock or soil, and 3) type of buried microorganism. These important variables, unfortunately, are not accounted for in the investigation made by Section V, Ref. 4.

It is proposed that effort be made to establish the functional form for \bar{f}_a , τ_1 and τ_2 in terms of the impact properties of spacecraft materials, properties of landing site and types of microorganism. Such an effort, however, needs extensive experimental data for verification.

2. Microbial release due to erosion. The release probability of a microorganism from the spacecraft, denoted by P_e , resulting from erosion can be formulated as follows:

$$P_e = M_{SI} P_{SI}(e|s) \cdot P(s) + M_m P_m(e|s) P(s) + M_b P_b(e|s) P(s) \quad (9)$$

where

$P_{SI}(e|s)$ = probability of release of a microorganism existing on the interior surface, resulting from erosion, given a soft landing

$P_m(e|s)$ = same definition as above for microbe on the mated surface

$P_b(e|s)$ = same definition as above for buried microbe

Since the probability of soft landing $P(s)$ is approximately 1.0, Eq. (9) can be written as

$$P_e \approx M_{SI} P_{SI}(e|s) + M_m P_m(e|s) + M_b P_b(e|s) \quad (10)$$

It is mentioned that $P_{SI}(e|s)$ and $P_m(e|s)$ have not been investigated in literature. $P_b(e|s)$ was formulated in Section V, Ref. 4 as follows:

$$P_b(e|s) = e_i \cdot f_o \cdot t \cdot P(e) \quad (11)$$

where

$$e_i \cdot f_o \cdot t \leq 1.0$$

e_i = erosion rate of spacecraft materials

f_o = initial fracture ratio

t = the period of time during which the material is subjected to erosion

$P(e)$ = probability that a buried microorganism survives the erosion process

The greatest uncertainties involved in the formulation are the erosion rate e_i and the survival probability $P(e)$. The erosion rate actually depends on the wind velocity and the size of particles impacting the landing material. Since both the particle size and the wind velocity are statistical quantities, $e_i P(e)$ should be written as follows:

$$e_i P(e) = \int_0^\infty \int_0^\infty e_i(x, y) P(e, x, y) f_1(x) f_1(y) dx dy \quad (12)$$

where $e_i(x, y)$ is the erosion rate given a particle size x and a wind velocity y , $f_1(x)$ and $f_2(y)$ are, respectively, the probability densities of the particle size and the wind velocity. $P(e, x, y)$ and $e_i(x, y)$ also depend on the landing materials, particle materials and the type of microorganism. This kind of approach is believed to be more rational than the approach used in Section V, Ref. 4.

5.2.1.4 Sterilization Environments. The reduction of microbial burden under sterilization environments, such as heat cycles and radiation, has been investigated extensively by Sandia Laboratory (Section V, Ref. 6). The analytical models established by Sandia for the effect of heat cycles and radiation, and the

combined effect of both are simple and reasonable. The effect of inhomogeneity of microorganisms with respect to the heat resistance was taken into account by assuming that the distribution of D value is lognormal. Considerable amount of experimental data has been generated to justify the analytical models. The general conclusion regarding the Sandia research is that the work they have done is good. There are many aspects in this area which have not been investigated by Sandia. These are listed in the following:

- 1) The effect of inhomogeneity in radiation resistance has not been taken into account.
- 2) The effect of inhomogeneity in resistance to the simultaneous application of heat and radiation has not been investigated.
- 3) The uncertainties associated with the dispersion of D value at each time instant with respect to the sample size and inhomogeneity have not been investigated. This investigation is of vital importance in providing the information for the analysis of confidence level associated with the final contamination probability estimate as discussed at the beginning of Section V.
- 4) The effect of sterilization environments on the reduction of microbial burden existing on the mated surface or buried in the materials has not been investigated. (Heat sterilization has been extensively investigated.)
- 5) The combined fractional reduction of microbial burden under various environments has not been investigated. For instance, the D value of a particular microorganism is a function of the temperature T, denoted by D(T). Suppose the microorganism is subjected to a sequence of temperatures T_1, T_2, \dots, T_N , respectively, for periods of time t_1, t_2, \dots, t_N . A possible expression for the fractional reduction could be written as

$$\exp \left\{ - \sum_{i=1}^N t_i / D(T_i) \right\}$$

The above expression implies that the order of application of the sequence of environments does not effect the final fractional reduction of microbial burden. This implication may or may not be true. Experimental verification would be required.

- 6) The approach to deal with the situation when the spectra of environments are random variables, e.g., T_1, T_2, \dots, T_N and t_1, t_2, \dots, t_N are random variables, has not been established.

Problems listed above, which have not been investigated in the literature, are believed to have significant bearing on the derivation of microbial reduction under space radiation (see Fig. 5-A.1). The spectra of radiations in space, such as the strength, dosage and durations of protons and electrons, are, in fact, random variables.

5.2.2 Approach for Microbial Burden Prediction

In Section V, Ref. 8, a considerable amount of microbial data, e.g., data from the Mariner 71 series (flight 1, flight 2, and PTM), has been compiled and analyzed. The compound Poisson Model was employed to fit the data. The author concluded that the compound Poisson Model did not fit the data. No further attempt was made to establish a better statistical model in Ref. 8, although such establishment is of vital importance as discussed in the literature. The first part of this subtask suggests a statistical model called "Negative Binomial Distribution". This model (para. 5.2.2.1) is expected to more closely fit the data.

In Section V, Ref. 9, expressions for the microbial burden in terms of a number of random variables was simulated by solving the equation for birth and death process (see para. 5.2.2.2). The distribution of microbial burden as a function of time is then estimated by use of a so-called "histogram operation". The histogram operation approach, however, has no mathematical basis and is an "arbitrary" procedure rather than a rational approximation. Hence, the meaningfulness of the final estimated histogram is in question, despite the fact that it is a tedious numerical operation. The second part of this subtask proposes the use of a simple, rational approach called "method for generating system moments" (Section V, Ref. 10), in conjunction with the Pearson distribution (Section V, Refs. 11-12). Advantages pertinent to the proposed method are discussed in detail.

5.2.2.1 Negative Binomial Model. It is well known that the Poisson distribution is the limiting case of the Binomial distribution which represents the outcome of independent trials. The assumption of independent trial is quite reasonable for the bioburden. However, both the Poisson and Binomial distributions are one parameter systems which do not allow sufficient degree of freedom to fit the data. For instance, the statistical dispersion of the Poisson distribution is $1/\sqrt{\lambda}$ where λ is the mean value. Therefore, the Negative Binomial distribution which contains two parameters is suggested in the following:

$$P_r[X = x] = \binom{x+s-1}{x} p^s (1-p)^x \quad (13)$$

$$x = 0, 1, 2, \dots$$

in which X represents the number of viable particles, s and p are parameters determined by fitting the data. The mean value μ_1 , and the variance μ_2 of this distribution can be obtained as:

$$\mu_1 = \frac{s(1-p)}{p} \quad (14)$$

$$\mu_2 = \frac{s(1-p)}{p^2} \quad (15)$$

5.2.2.2 Microbial Burden Model. The microbial burden B resulting from events of fallout, contact and decontamination can be expressed as (Section V, Ref. 9)

for fallout

$$B = B_o e^{-t/V} + AV f_2 g(C + Q) [1 - e^{-t/V}] \quad (16)$$

for contact

$$B = B_o \left(1 - \frac{aS_2}{2A} \right) + \frac{aS_1 b_t}{2} \quad (17)$$

for decontamination

$$B = B_o (1 - k_j) \quad (18)$$

in which B and B_o are bioburdens after and before the event, respectively, and t denotes the time. The meaning of other quantities appearing in Eqs. (16-18) are given in Section V, Ref. 9. It is pointed out here that B_o , V , f_2 , g , C , Q , A , S_1 , S_2 , b_t and k_j are all statistical random variables from which the statistical distribution of bioburden B should be estimated through Eqs. (15-18). As noted previously, the meaning of the final distribution of B , using the "histogram approach", is subject to question.

The approach proposed herein is by use of the method for generating system moments (Section V, Ref. 10). Then, based on estimates of the first four central moments, a Pearson distribution (Section V, Refs. 11-12) approximation can be used to estimate the statistical distribution of bioburden B at each time instant t . Since the Pearson system includes many diverse distributions (Section V, Refs. 11-12) this method usually leads to an adequate approximation. The method is sometimes referred to as statistical error propagation (Section V, Ref. 10).

1. Generation of moments. Let the relationship between the system variable Z and the component variables, x_1, x_2, \dots, x_n , be given by the function

$$Z = h(x_1, x_2, \dots, x_n) \quad (19)$$

For example, in the case of bioburden, Z represents the bioburden B and $h(x_1, x_2, \dots, x_n)$ is given by Eqs. (16-18).

Let $E(x_i)$ be the mean or expected value for the i^{th} component variable and let $\mu_i(x_b)$ denote its k^{th} central moment (or moment about the mean).

Similarly, $E(Z)$ and $\mu_k(Z)$ denote the expected value and the k^{th} moment about the mean for system variable, respectively. The problem is to obtain an estimate of $E(Z)$ and $\mu_k(Z)$ for $k = 2, 3$, and 4 , based on 1) data on the component variables from which estimates of $E(x_i)$ and $\mu_k(x_i)$ for $i = 1, 2, \dots, n$ can be obtained and 2) knowledge of the system function $h(x_1, x_2, \dots, x_n)$, i.e., Eq. (19).

The method consists of expanding $h(x_1, x_2, \dots, x_n)$ about $[E(x_1), E(x_2), \dots, E(x_n)]$, the point at which each of the component variables takes on its expected value, by a multivariable Taylor series. An equation for the expected value of system variable is then obtained by taking expected values in the resulting expression and applying some simple algebra. The complete derivation is given in Section V, Ref. 10. Assuming that the component variables are uncorrelated, the final expression for mean system variable Z , retaining terms up to second order, is

$$E(Z) = h[E(x_1), E(x_2), \dots, E(x_n)] + \frac{1}{2} \sum_{i=1}^n \frac{\partial^2 \bar{h}}{\partial x_i^2} E(x_i) \quad (20)$$

where $\partial^2 \bar{h} / \partial x_i^2$ denotes $\partial^2 h / \partial x_i^2$ evaluated at $E(x_r)$ that is, with the $E(x_r)$ substituted for x_r for $r = 1, 2, \dots, n$. For example, if $h(x_1, x_2, x_3) = x_1^2 x_2^3 x_3$

$$\frac{\partial^2 \bar{h}}{\partial x_3^2} = E(x_1) E^2(x_2) [6E(x_3)] \quad (21)$$

Henceforth, $\partial^2 \bar{h} / \partial x_i^2$ is written without the bar on h — that is, as $\partial^2 h / \partial x_i^2$. Equation (20) requires knowledge or estimates of the means and variances for each of the component variables.

Note that estimating $E(Z)$ by substituting the component means into the system equation; that is, setting

$$E(Z) = h[E(x_1), E(x_2), \dots, E(x_n)] \quad (22)$$

provides an exact result only when all second and higher order partial derivatives are zero; otherwise Eq. (22) is an approximation.

The Taylor-series expansion for the variance of system variable Z , assuming the component variables to be uncorrelated, is derived in Section V, Ref. 10. The resulting equation, retaining terms up to third order, reduces to

$$\mu_2(Z) = \sum_{i=1}^n \left(\frac{\partial h}{\partial x_i} \right)^2 \mu_2(x_i) + \sum_{i=1}^n \left(\frac{\partial h}{\partial x_i} \right) \left(\frac{\partial^2 h}{\partial x_i^2} \right) \mu_3(x_i) \quad (23)$$

Expressions for the third and fourth central moments for the system variable, that is $\mu_3(Z)$ and $\mu_4(Z)$, may be derived in a manner analogous to that for the variance. The resulting expressions, retaining only the lowest-order nonzero terms, are

$$\mu_3(Z) = \sum_{i=1}^n \left(\frac{\partial h}{\partial x_i} \right)^3 \mu_3(x_i) \quad (24)$$

$$\mu_4(Z) = \sum_{i=1}^n \left(\frac{\partial h}{\partial x_i} \right)^4 \mu_4(x_i) + 6 \sum_{i=1}^n \sum_{j=1, j \neq i}^n \left(\frac{\partial h}{\partial x_i} \right)^2 \left(\frac{\partial h}{\partial x_j} \right)^2 \mu_2(x_i) \mu_2(x_j) \quad (25)$$

All derivatives are again evaluated at the mean values of the variates.

Up to this point the component variables have been assumed to be uncorrelated. Correlation between components occurs when the random value taken by one or more components in a system is related to the random value of one or more other components in the same system. Expressions for system variable Z when component variables are correlated can be obtained in a fashion analogous to the uncorrelated case (see Section V, Ref. 10).

2. Discussion of the method. The method of generating system moments is an approximate, rather than an exact, procedure, because of the omission of higher-order terms in the Taylor series expansion. A study of the general adequacy of the method (Section V, Ref. 10) concluded that the approximation is very satisfactory and that the retention of only the lowest order terms is frequently adequate. Ref. 10 also gives expressions which include additional higher order terms for the mean and for the second, third, and fourth central

moments for both the uncorrelated and correlated cases. These expressions can be used when still greater precision is required.

It should be emphasized that the mean, variance, and central moments of component variables, x_1, x_2, \dots, x_n are estimated from test data thus involving sampling errors. Unless a considerable amount of test data is available such a sampling error may well exceed that introduced by omission of higher order terms. This may be the case in the practical situation.

Advantages pertinent to the application of method of generation of moments can be summarized as follows:

- 1) The generation of system moments allows us to analyze the relative importance of each component variable by examining the magnitude of its partial derivative. As a result, it might be desirable to set more stringent tolerances on those components that contribute most heavily to the system variance.
- 2) The generation of system moments does not necessarily require any assumptions concerning the form of the component distributions. Only the estimates of the moments of the component variables were required, rather than the complete component distributions.

In conclusion, the bioburden distribution based on component information can be drawn conveniently from the method of generation of system moments described herein, in conjunction with the Pearson distribution (Section V, Ref. 11). The method provides a reasonable and more refined approach than the method of histograms, since the derivatives of the system function can easily be obtained.

5.2.3 Approach for Analyzing the Vacuum Temperature Data

Data from the Natural Space Environment Task's vacuum temperature experiment was analyzed to determine if a reduction function could be derived from the results. The analysis was performed in three phases: Phase one was the raw data analysis, including determination of the reduction ratio and formulation of both a normal and lognormal model; Phase two was the analytical formulation of a least squares fit of the data; and Phase three, currently in progress, is to develop a computer program based on the results of Phases one and two. The mathematical formulations resulting from phases one and two are given in the Appendix.

5.2.4 Theoretical Formulation for Planetary Quarantine Standards

During this reporting period, a paper was written pertaining to the theoretical formulation of the planetary quarantine standards and optimum sterilization strategy. The abstract for the paper is given below:

"A general analytical formulation for planetary contamination is presented herein. Upper and lower bounds of the contamination probability are established. The formulation is more general than that currently available in literature in the sense that, during the quarantine period, each mission is not assumed to be identical. Advantages and physical implications associated with upper and lower bounds of contamination probability are discussed in detail. Based on the new formulation for planetary contamination, a sequential optimum sterilization strategy is formulated which determines the optimum allocation of contamination probability to each mission such that the total cost of sterilization is minimized, while the constraints on the overall contamination probability is satisfied. This sequential optimization scheme incorporates the information obtained from previous missions into the subsequent mission. Numerical results indicate that the optimum strategy results in a significant saving in sterilization cost over the current practice."

5.3 CONCLUSIONS

The following summarizes the conclusions from the probability estimation methods and analysis task:

- 1) The estimation methods and analytical models used by the planetary quarantine community are basically sound. However, some of these methods and models can be made more mathematically rigorous by restructuring their formulation. Analytical restructuring has been developed for microbial burden prediction (paragraph 5.2.2) and planetary contamination (paragraph 5.2.4).
- 2) Several parameters discussed in the models require experimental data for verification or refinement (see pp. 5-4, 5-8, 5-12, 5-13).
- 3) An approach for analyzing the vacuum temperature data, based on a lognormal model and a least squares fit, was developed. It is recommended that analogous techniques be applied to the biological data resulting from the Natural Space Environment Studies.

5.4 PROBLEM AREAS

No problems were encountered during this reporting period.

5.5 FUTURE ACTIVITIES

Because of FY '73 reprogramming, this task was terminated in January, 1973.

5.6 PRESENTATIONS

Yang, J. "Theoretical Formulation of Planetary Quarantine Standards", presented at Viking PQ Analysis Review, February 14, 1973 at JPL.

5.7 PUBLICATIONS

Yang, J. and Hoffman A., "Theoretical Formulation for Planetary Quarantine Standards and Optimum Sterilization Strategy", (in preparation).

REFERENCES

1. Schalkowsky, S., and Jacoby, I., "Safety Margins in the Implementation of Planetary Quarantine Requirements," COSPAR Identification # P.Q. 5.
2. Roark, A.L., "A Stochastic Bioburden Model for Spacecraft Sterilization", Space Life Sciences, Vol. 3, pp. 239-253, 1972.
3. Bharucha-Reid, Elements of the Theory of Markov Processes and Their Applications, McGraw-Hill, 1960.
4. "Evaluation of Microbial Release Probabilities", Interim Report, Contract NASW-2062, Exotech Systems, Inc., Washington, D.C., April 1972.
5. Gustan, E.A., and Olson, R.L., "Release of Microorganisms from Solid Materials," Final Report prepared for Jet Propulsion Laboratory, July 1971, The Boeing Company, Aerospace Group, Seattle, Washington.
6. "Final Report of Planetary Quarantine Activities," SC-RR-72 0516, Planetary Quarantine Department, Sandia Laboratory, August, 1972.
7. Parzon, E., Stochastic Processes, Holden-Day, Inc., 1964.
8. Efron, B., "Analysis of Microbial Burden Data" Appendix A, Planetary Quarantine Annual Review July 71-July 73, 900-597, Jet Propulsion Laboratory, February, 1973.
9. Hoffman, A.R., and Winterburn, D.A., "Microbial Burden Model for Unmanned Planetary Spacecraft," Final Report, 900-566, Jet Propulsion Laboratory, June 30, 1972.
10. Tukey, J.W., Statistical Techniques Research Group, Princeton University, Princeton, New Jersey, Technical Reports 10, 11, and 12: (10) "The Propagation of Errors, Fluctuations and Tolerances-Basic Generalized Formulas"; (11) "The Propagation of Errors, Fluctuations and Tolerances-Supplementary Formulas"; (12) "The Propagation of Errors, Fluctuations and Tolerances-An Exercise in Partial Differentiation."
11. Elderton, W.P., Frequency Curves and Correlation, 4th ed., Cambridge University Press, Cambridge, 1953.
12. Johnson, N.L., Nixon, E., and Amos, D.E., "Table of Percentage Points of Pearson Curves, for Given $\sqrt{\beta_1, \beta_2}$, Expressed in Standard Measure," Biometrika, Vol. 50, p. 459, 1963.

APPENDIX A

ANALYTICAL APPROACH FOR ANALYZING
THE VACUUM TEMPERATURE DATA

This appendix presents the mathematical formulation that forms the basis for analyzing the vacuum temperature data which resulted from the Natural Space Environment task. Para. A-1 gives the results of Phase 1 of this probability estimation subtask which pertained to the approach for analyzing the raw data. Para. A-2, representing Phase 2, gives the analytical formulation of the least squares fit of the data.

A.1 APPROACH FOR ANALYZING THE RAW DATA

Let

$X_i(t_j, T_\ell)$ = Number of colonies on tack i at sampling time t_j , and temperature T_ℓ

$$i = 1, 2, \dots, N_{j\ell}$$

$$j = 1, 2, \dots, J$$

$$\ell = 1, 2, \dots, L$$

where

$N_{j\ell}$ = Number of tacks for sampling at time t_j and temperature T_ℓ

J = Number of sampling times

L = Number of sampling temperatures

A.1.1 Normal Model

$X_i(t_{jo}, T_o)$ = Number of colonies on tack i at room temperature

$$\bar{X}(t_{jo}, T_o) = \frac{1}{N_j} \sum_{i=1}^{N_j} X_i(t_{jo}, T_o)$$

N_j = Number of tacks for sampling at room temperature at t_o for
 t_j sampling

The raw data is normalized to the room temperature at t_o by setting

$$x_i(t_j, T_\ell) = \frac{X_i(t_j, T_\ell)}{\bar{X}(t_{jo}, T_o)}$$

(Note that the subscripts of the left hand member are the same as the subscripts of the numerator of the right hand member.)

Define

$\bar{x}(t_j, T_\ell)$ = estimated mean value of tack counts at sampling time t_j
 and temperature T_ℓ

and

$s(t_j, T_\ell)$ = estimated standard deviation of tack counts at sampling
 time t_j and temperature T_ℓ .

Then, the mean is calculated

$$\bar{x}(t_j, T_\ell) = \frac{1}{N_{j\ell}} \sum_{i=1}^{N_{j\ell}} x_i(t_j, T_\ell) .$$

The variance is

$$\begin{aligned} s^2(t_j, T_\ell) &= \frac{1}{N_{j\ell} - 1} \sum_{i=1}^{N_{j\ell}} \left[x_i(t_j, T_\ell) - \bar{x}(t_j, T_\ell) \right]^2 \\ &= \frac{\sum_{i=1}^{N_{j\ell}} x_i^2(t_j, T_\ell)}{N_{j\ell} - 1} - \frac{N_{j\ell}}{N_{j\ell} - 1} \bar{x}^2(t_j, T_\ell) . \end{aligned}$$

And finally the standard deviation is

$$s(t_j, T_\ell) = \sqrt{s^2(t_j, T_\ell)} .$$

Let

$$V(t_j, T_\ell) = \text{coefficient of variation (dispersion),}$$

where

$$V(t_j, T_\ell) = \frac{s(t_j, T_\ell)}{\bar{x}(t_j, T_\ell)} .$$

Assuming that the tack count is normally distributed, the confidence interval is as follows

$$\left[L(t_j, T_\ell), U(t_j, T_\ell) \right] = \left[\bar{x}(t_j, T_\ell) - \frac{ks(t_j, T_\ell)}{\sqrt{N_{j\ell}}}, \bar{x}(t_j, T_\ell) + \frac{ks(t_j, T_\ell)}{\sqrt{N_{j\ell}}} \right]$$

where k is the parameter associated with confidence level α , which is obtained from the $\alpha/2$ 100 percentage point of Student's t -distribution or from the following formula,

$$k \approx \chi \left[1 + \frac{\chi^2 + 1}{4(N_{j\ell} - 1)} + \frac{(\chi^2 + 3)(5\chi^2 + 1)}{96(N_{j\ell} - 1)^2} \right]$$

where χ is the $\alpha/2$ times one hundred percentage point of normal distribution. It is 1.96 for $\alpha = 95$ percent.

The initial conditions for the normal model are calculated as follows.

From the normalization relation

$$x_i(t_{jo}, T_o) = \frac{X_i(t_{jo}, T_o)}{\bar{X}(t_{jo}, T_o)} .$$

Let

$$M = \sum_{j=1}^J N_j .$$

Then

$$\bar{x}(t_o, T_o) = \frac{1}{M} \sum_{j=1}^J \sum_{i=1}^{N_j} x_i(t_{jo}, T_o) ,$$

and the variance is

$$s^2(t_o, T_o) = \frac{1}{M-1} \sum_{j=1}^J \sum_{i=1}^{N_j} \left[x_i(t_{jo}, T_o) - \bar{x}(t_o, T_o) \right]^2 .$$

The coefficient of variation

$$V(t_o, T_o) = \frac{s(t_o, T_o)}{\bar{x}(t_o, T_o)} .$$

And the confidence interval is

$$\left[\bar{x}(t_o, T_o) - \frac{ks(t_o, T_o)}{\sqrt{M}} , \bar{x} + \frac{ks(t_o, T_o)}{\sqrt{M}} \right] .$$

A.1.2 Lognormal Model

The logarithmic transformation of the room temperature data at time t_o for the t_j sampling is

$$Y_i(t_{jo}, T_o) = \log_{10} X_i(t_{jo}, T_o) .$$

The estimate of the mean is

$$\bar{Y}(t_{jo}, T_o) = \frac{1}{N_j} \sum_{i=1}^{N_j} Y_i(t_{jo}, T_o) .$$

For the raw data, \bar{Y} would be the geometric mean.

The note at the end of this section shows that

$$\hat{X}(t_{jo}, T_o) = \text{median} = 10^{\bar{Y}(t_{jo}, T_o)}$$

To factor out the initial condition variation, each data point is normalized by the median of the initial conditions and the quotient subjected to a logarithmic transformation.

$$\begin{aligned} y_i(t_j, T_\ell) &= \log \frac{X_i(t_j, T_\ell)}{\hat{X}(t_{jo}, T_o)} \\ &= \log X_i(t_j, T_\ell) - \bar{Y}(t_{jo}, T_o) . \end{aligned}$$

Then the mean is calculated

$$y(t_j, T_\ell) = \frac{1}{N_{j\ell}} \sum_{i=1}^{N_{j\ell}} y_i(t_j, T_\ell) .$$

The variance is

$$\begin{aligned}
 s_y^2(t_j, T_\ell) &= \frac{1}{N_{j\ell} - 1} \sum_{i=1}^{N_{j\ell}} [y_i(t_j, T_\ell) - \bar{y}(t_j, T_\ell)]^2 \\
 &= \frac{1}{N_{j\ell} - 1} \sum_{i=1}^{N_{j\ell}} y_i^2(t_j, T_\ell) - \frac{N_{j\ell}}{N_{j\ell} - 1} \bar{y}^2(t_j, T_\ell) \quad .
 \end{aligned}$$

Let

$$\hat{y}(t_j, T_\ell) = \text{median} \quad .$$

Therefore

$$\hat{y}(t_j, T_\ell) = {}_{10}\bar{y}(t_j, T_\ell)$$

and the confidence interval for the median $\hat{y}(t_j, T_\ell)$ is

$$\left[{}_{10}\bar{y}(t_j, T_\ell) - {}_{10}ks_y(t_j, T_\ell)/\sqrt{N_{j\ell}}, {}_{10}\bar{y}(t_j, T_\ell) + {}_{10}ks_y(t_j, T_\ell)/\sqrt{N_{j\ell}} \right]$$

Coefficient of variation for lognormal model is the same as that for normal model. If the normal model is not computed, the coefficient of variation can be obtained as follows:

$$V^2(t_j, T_\ell) = e^{s_y^2(t_j, T_\ell)(\ln 10)^2} - 1$$

The initial conditions for the lognormal model are calculated as follows.

From the normalization relation

$$\begin{aligned} y_i(t_{j0}, T_o) &= \log \frac{X_i(t_{j0}, T_o)}{\hat{X}(t_{j0}, T_o)} \quad . \\ &= \log X_i(t_{j0}, T_o) - \bar{Y}(t_{j0}, T_o) \quad . \end{aligned}$$

Let

$$M = \sum_{j=1}^J N_j \quad .$$

Then

$$\bar{y}(t_o, T_o) = \frac{1}{M} \sum_{j=1}^J \sum_{i=1}^{N_j} y_i(t_{j0}, T_o) \quad ,$$

and

$$\hat{y}(t_o, T_o) = 10^{\bar{y}(t_o, T_o)} \quad .$$

The variance is

$$s_y^2(t_o, T_o) = \frac{1}{M-1} \sum_{j=1}^J \sum_{i=1}^{N_j} \left[y_i(t_{j0}, T_o) - \bar{y}(t_o, T_o) \right]^2$$

The coefficient of variation

$$V^2(t_o, T_o) = \exp \left\{ s_y^2(t_o, T_o) (\ln 10)^2 \right\} - 1 .$$

And the confidence interval is

$$\left[10^{\bar{y}(t_o, T_o) - ks(t_o, T_o)/\sqrt{M}}, 10^{\bar{y}(t_o, T_o) + ks(t_o, T_o)/\sqrt{M}} \right]$$

The lognormal model fits the experimental data better than the normal model. Consequently, it is the model being used for the data analysis.

NOTE

Prove that the median from a lognormal random variable can be derived from the mean.

Suppose

$$Y = \log_a X$$

where

X = logarithm of normal random variable

Y = normal random variable

Let

$$\bar{Y} = \text{mean of } Y$$

and

$$\hat{X} = \text{median of } X$$

For the median, by definition,

$$\frac{1}{2} = F(\hat{X}) = P(X \leq \hat{X}) = P(\log X \leq \log \hat{X}) .$$

By substituting for Y

$$\frac{1}{2} = P(Y \leq \log \hat{X}) . \quad (\text{Equation 1})$$

For a normal random variable, the

$$\text{mean} = \text{median}$$

Therefore,

$$\frac{1}{2} = P(Y \leq \bar{Y}) .$$

Setting Eq. (1) equal to Eq. (2),

$$P(Y \leq \log \hat{X}) = P(Y \leq \bar{Y}) .$$

$$\therefore \bar{Y} = \log \hat{X}$$

or equivalently,

$$\hat{X} = \text{antilog } \bar{Y} = 10^{\bar{Y}} .$$

A.2 METHOD OF LEAST SQUARES

A.2.1 Roark and Reynolds Model (Ref. 1)

Let

$X(t)$ = Number of survivors at time t ,

$p(t)$ = Probability of single organism survival at time t ,

$\bar{X}(t)$ = Mean value of $X(t)$.

The basic assumption is that the survival of each microorganism is statistically independent.

$$P[X(t) = k | X(0) = N_o] = \binom{N_o}{k} p^k(t) [1 - p(t)]^{N_o - k} \quad (1)$$

$$\begin{aligned} P[X(t) = k] &= \sum_{N_o=0}^{\infty} P[X(t) = k | X(0) = N_o] P[X(0) = N_o] \\ &= \sum_{N_o=0}^{\infty} \binom{N_o}{k} p^k(t) [1 - p(t)]^{N_o - k} P[X(0) = N_o] \end{aligned} \quad (2)$$

$$E[X(t)] = E[X(0)] p(t) \quad (3)$$

$$\bar{X}(t) = \bar{X}(0) p(t) \quad (4)$$

Let

$$Y(t) = \log \bar{X}(t) . \quad (5)$$

Then, from Eq. (4),

$$Y(t) = Y(0) + \log p(t) . \quad (6)$$

Set

$$p(t) = 10^{-t/D} \quad (7)$$

From Eq. (6),

$$Y(t) = Y(0) - \gamma t + \epsilon \quad (8)$$

where

$$\gamma = 1/D$$

ϵ = observation error introduced to account for the variation of tack count.

It is assumed that

- 1) ϵ is independent of time
- 2) ϵ is normally distributed

$$E[\epsilon] = 0, E[\epsilon^2] = \sigma_\epsilon^2$$

The following summarizes the applicability of the Roark-Reynolds model.

- 1) The model accounts for the case $p(t) = 10^{-t/D}$ only. The actual situation is $p(t, T)$ or $p(t, T, I)$ where t , T , and I represent, respectively, time, temperature and type of microorganism.
- 2) ϵ is independent of time. This is not true for the vacuum temperature experiment. ϵ depends on time and temperature.
- 3) Introduction of normal error, ϵ , associated with log mean observation is too artificial. In the JPL experiments, this variation comes from the fact that the number of microorganisms on the tack is a random variable.

A.2.2 Yang Model

A.2.2.1 Introduction. It is assumed that there exists a reduction function for the microorganisms when subjected to environmental stresses, such as vacuum and temperature.

Mathematically,

$$X(t, T) = X(t_0, T_0) f(t, T) \quad (9)$$

where

$X(t, T)$ = Number of microorganisms at time t and temperature T

$X(t_0, T_0)$ = Number of microorganisms at the initial condition

$f(t, T)$ = function of time and temperature representing the probability of survival of $X(t_0, T_0)$. This is the function to be estimated.

Equation (9) is more general than Eq. (4) since it degenerates into Eq. (4) when the average operation is taken.

For the actual experiment, one cannot count $X(t_0, T_0)$ nor $X(t, T)$ deterministically. The experimental procedure is to count $X(t, T)$ from samples of tacks whose counts $X(t_0, T_0)$ at $t = t_0$, $T = T_0$ are not known. The number of counts on tacks is a random variable. Therefore, $X(t, T)$ is a random variable resulting from the random variable $X(t_0, T_0)$.

Dividing Eq. (9) by $\hat{X}(t_0, T_0)$, one obtains

$$\frac{X(t, T)}{\hat{X}(t_0, T_0)} = \frac{X(t_0, T_0)}{\hat{X}(t_0, T_0)} f(t, T) \quad (10)$$

where $\hat{X}(t_0, T_0)$ is the median of $X(t_0, T_0)$.

Equation (10) can be written as

$$Y(t, T) = Y(t_o, T_o) + \log f(t, T) \quad (11)$$

where

$$\left. \begin{aligned} Y(t, T) &= \log \frac{X(t, T)}{X(t_o, T_o)} \\ Y(t_o, T_o) &= \log \frac{X(t_o, T_o)}{X(t_o, T_o)} \end{aligned} \right\} \quad (12)$$

It is reasonable to assume that the distribution of the microbial count $X(t, T)$ and $X(t_o, T_o)$ are lognormal. Therefore, $Y(t, T)$ is a normal random variable; $Y(t_o, T_o)$ is a normal random variable with mean zero and is designated by $\epsilon(t_o, T_o)$.

Hence, Eq. (11) can be written as

$$Y(t, T) = \log f(t, T) + \epsilon(t_o, T_o) \quad (13)$$

Assume that

$$f(t, T) = 10^{\alpha_o + \alpha_1 t g_1(T) + \alpha_2 t^2 g_2(T) + \dots + \alpha_m t^m g_m(T)} \quad (14)$$

where $g_j(T)$ is a suitable function of T .

Then, Eq. (13) becomes

$$Y(t, T) = \alpha_o + \alpha_1 t g_1(T) + \alpha_2 t^2 g_2(T) + \dots + \alpha_m t^m g_m(T) + \epsilon(t_o, T_o) \quad (15)$$

The estimation of $\alpha_0, \alpha_1, \alpha_2, \dots, \alpha_m$ for the model of Eq. (15) will be discussed in conjunction with the experimental data.

A.2.2.2 Solution by method of least square. The Yang model can be summarized as follows

- 1) The experimental observations give rise to n different quantities y_1, y_2, \dots, y_n .
- 2) Each of these n observations is known to depend linearly on a set of $m \leq n$ parameters $\alpha_1, \alpha_2, \dots, \alpha_m$.
- 3) There is a random variable ϵ_i associated with each observation z_i so that the observational equation can be written

$$\left. \begin{aligned} y_1 &= A_{11} \alpha_1 + A_{12} \alpha_2 + \dots + A_{1m} \alpha_m + \epsilon_1 \\ y_2 &= A_{21} \alpha_1 + A_{22} \alpha_2 + \dots + A_{2m} \alpha_m + \epsilon_2 \\ &\vdots \\ y_n &= A_{n1} \alpha_1 + A_{nm} \alpha_m + \dots + A_{nm} \alpha_n + \epsilon_m \end{aligned} \right\} \quad (16)$$

In matrix form

$$\underline{\underline{Y}} = \underline{\underline{A}} \underline{\underline{\alpha}} + \underline{\underline{\epsilon}} \quad (17)$$

where

$$\underline{\underline{Y}} = \begin{bmatrix} y_1 \\ y_2 \\ \vdots \\ y_n \end{bmatrix}, \quad \underline{\underline{\alpha}} = \begin{bmatrix} \alpha_1 \\ \alpha_2 \\ \vdots \\ \alpha_m \end{bmatrix}, \quad \underline{\underline{\epsilon}} = \begin{bmatrix} \epsilon_1 \\ \epsilon_2 \\ \vdots \\ \epsilon_n \end{bmatrix} \quad (18)$$

$$\tilde{A} = \begin{bmatrix} A_{11} & A_{12} & A_{13} & \dots & A_{1m} \\ A_{21} & A_{22} & A_{23} & \dots & A_{2m} \\ \vdots & \vdots & \vdots & \dots & \vdots \\ A_{n1} & A_{n2} & A_{n3} & \dots & A_{nm} \end{bmatrix} \quad (19)$$

Let

$$\sigma_2^v = E \left[\epsilon_i^2 \right] ; \quad i = 1, 2, \dots, n \quad , \quad (20)$$

$$\tilde{M}_y = \begin{bmatrix} \sigma_1^2 & 0 & 0 & \dots & 0 \\ 0 & \sigma_2^2 & 0 & \dots & 0 \\ 0 & 0 & \sigma_3^2 & \dots & 0 \\ \vdots & \vdots & \vdots & \ddots & \vdots \\ 0 & 0 & 0 & \dots & \sigma_n^2 \end{bmatrix} \quad (21)$$

The observations are assumed to be independent.

By the method of least square, the estimate of α , denoted by $\hat{\alpha}$, can be shown to be

$$\hat{\alpha} = \left(\tilde{A}^T \tilde{M}_y^{-1} \tilde{A} \right)^{-1} \tilde{A}^T \tilde{M}_y^{-1} \tilde{Y} \quad (22)$$

and hence

$$\hat{\tilde{Y}} = \tilde{A} \hat{\alpha} \quad (23)$$

The standard deviation of the error of the estimated vector, $\hat{\tilde{Y}}$, that is

$$\hat{\tilde{Y}} - \tilde{Y}^0 = \tilde{A} \hat{\alpha} - \tilde{A} \alpha = \tilde{A} (\hat{\alpha} - \alpha) \quad (24)$$

where

$$\tilde{Y}^0 = E[\tilde{Y}] = \tilde{A} \alpha$$

The mean value of \tilde{Y} is defined as \tilde{Y}^0 ,

$$\tilde{Y}^0 \equiv E[\tilde{Y}] \equiv \tilde{A} \alpha , \quad (25)$$

$$\begin{aligned} \tilde{\sigma}^2 &= E\left[(\hat{\tilde{Y}} - \tilde{Y}^0)(\hat{\tilde{Y}} - \tilde{Y}^0)^T\right] \\ &= E\left[\tilde{A}(\hat{\alpha} - \alpha)(\hat{\alpha} - \alpha)^T \tilde{A}^T\right] \\ &= \tilde{A} \tilde{B}^{-1} \tilde{A}^T , \end{aligned} \quad (26)$$

where

$$\tilde{B}^{-1} = \left(\tilde{A}^T \tilde{M}_y^{-1} \tilde{A} \right)^{-1} , \quad (27)$$

because

$$E\left[(\hat{\alpha} - \alpha)(\hat{\alpha} - \alpha)^T\right] = B^{-1} . \quad (28)$$

Since,

$$\hat{\alpha} = B^{-1} \tilde{A}^T \tilde{M}_y^{-1} \tilde{Y} , \quad (29)$$

and

$$E[\tilde{Y}] = \tilde{A} \alpha , \quad (30)$$

then

$$\begin{aligned} E[\hat{\underline{\alpha}}] &= \underline{\tilde{B}}^{-1} \underline{\tilde{A}}^T \underline{\tilde{M}}_y^{-1} \underline{\tilde{A}} \underline{\alpha} \\ &= \underline{\alpha} \end{aligned} \quad (31)$$

It follows from Eq. (29) that $\hat{\underline{\alpha}}$ is a normal vector since \underline{Y} is a normal vector. Therefore, $\hat{\underline{\alpha}}$ is a normal vector with mean value $\underline{\alpha}$ and standard deviation

$$\underline{\sigma}_{\underline{\alpha}}^2 = E[(\hat{\underline{\alpha}} - \underline{\alpha})(\hat{\underline{\alpha}} - \underline{\alpha})^T] = \underline{\tilde{B}}^{-1}.$$

Then, $\hat{\alpha}_j - \alpha_j / \sigma_{\alpha_j}$ is a normal random variable with zero mean and standard deviation one.

Therefore, the confidence interval for α_j is

$$[\hat{\alpha}_j - k \sigma_{\alpha_j}, \hat{\alpha}_j + k \sigma_{\alpha_j}]$$

where k is obtained from the normal table at $\alpha/2$ 100 percentage level.

Reference:

Hamilton, W.C., Statistics in Physical Science, Ronald Press Co., NY, 1964.